iScience

CellPress
OPEN ACCESS

Article

The SH3-binding domain of chorismate mutase protein of *Mycobacterium tuberculosis* contributes to mycobacterial virulence

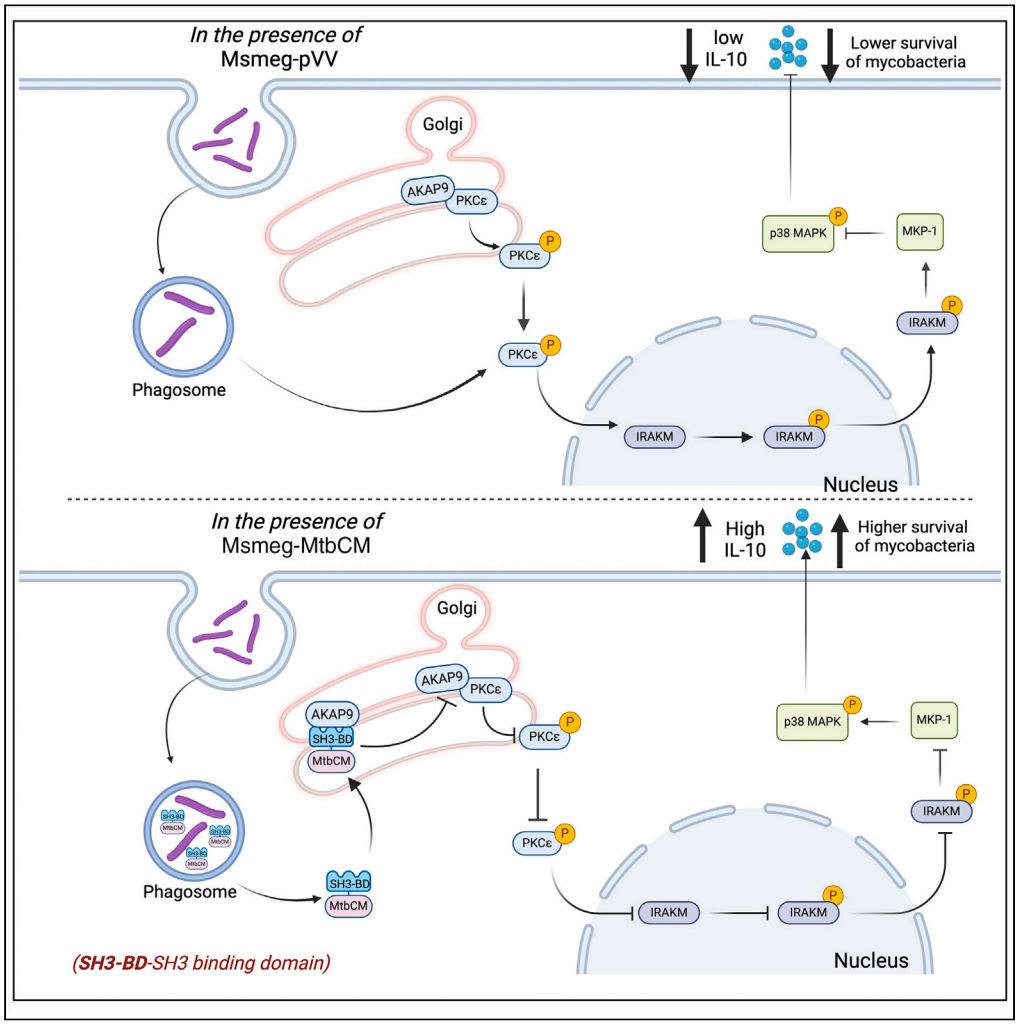

Ravi Pal, Vandana Maurya, Supriya Borah, Sangita Mukhopadhyay

sangita@cdfd.org.in

Highlights

Mtb chorismate mutase (MtbCM) acts as a virulence factor supporting bacterial growth

MtbCM targets AKAP9-PKCε-MKP-1-p38 MAPK signaling axis to activate a favorable IL-10

SH3-binding domain of MtbCM contributes to mycobacterial virulence

Pal et al., iScience 27, 111044
November 15, 2024
https://doi.org/10.1016/j.isci.2024.111044

iScience

CellPress
OPEN ACCESS

Article

The SH3-binding domain of chorismate mutase protein of *Mycobacterium tuberculosis* contributes to mycobacterial virulence

Ravi Pal,[1,2] Vandana Maurya,[1,3] Supriya Borah,[1] and Sangita Mukhopadhyay[1,4,*]

SUMMARY

Crystal structure of the secretory chorismate mutase protein of *Mycobacterium tuberculosis* (MtbCM) reveals presence of a proline rich region on its surface that serve as a recognition site for protein-protein interaction. This study shows that MtbCM upregulates IL-10 which favors *M. tuberculosis* by affecting PKCε-MKP-1-p38 MAPK signaling. MtbCM translocates to the Golgi-network where it interacts with AKAP9 via its SH3-binding domain to inhibit AKAP9-PKCε interaction and reducing PKCε phosphorylation. In the absence of phosphorylated PKCε, IRAK3 fails to stabilize MKP-1 resulting in higher p38 MAPK activation and IL-10 production. *M. smegmatis* expressing MtbCM survived better in infected mice. Mutation in SH3-binding domain ablated MtbCM-AKAP9 interaction resulting in IL-10 production and decreased bacterial survival. This study highlights the importance of SH3-binding domain in host-pathogen interaction and a role of MtbCM in modulation of cytokine response and mycobacterial virulence in addition to its role in shikimate pathway.

INTRODUCTION

Shikimate pathway is a multistep process for the synthesis of aromatic amino acids using carbohydrates (phosphoenolpyruvate and erythrose 4-phosphate) to chorismate.[1] The chorismate is further converted to prephenate by an enzyme called chorismate mutase. Chorismate mutase (CM) is one of the most important enzymes for aromatic amino acid biosynthesis found in microorganisms (bacteria and fungi) but absent in mammals.[2] It regulates the balance of aromatic amino acids inside the cell. Chorismate mutase catalyzes the conversion of chorismate to prephenate to form tyrosine and phenylalanine by subsequent action of prephenate dehydrogenase or prephenate dehydratase respectively.[3] Based on the structure, chorismate mutases can be classified into two major groups; AroH class (with trimeric pseudo α/β barrel structure) or AroQ class (with dimeric helix bundle structure).

Many pathogenic organisms like *Erwinia herbicola*, *Meloidogyne javanica*, *Rhodococcus equi*, and *Mycobacterium tuberculosis* (Mtb) possess secretory chorismate mutase.[1,4] During infection, *M. javanica* secretes chorismate mutase into plant vascular tissue and converts the plant cells into giant feeder cells with a multi-lobed nucleus.[5] In *Xanthomonas oryzae*, chorismate mutase attenuates intensity of the infection to deceive immune response of the plant and enables higher survival of the bacteria.[6] During *Salmonella typhimurium* infection, *aroQ*, encoding a putative *chorismate mutase*, and *pheA* encoding a bifunctional chorismate mutase/prephenate dehydratase involved in phenylalanine biosynthesis are highly expressed.[7] All these examples point to a critical role of chorismate mutase in the virulence of pathogens.

Despite the availability of curable drugs, tuberculosis (TB) is one of the leading causes of human death for decades. Genome sequencing of *M. tuberculosis* has identified two putative genes, Rv1885c and Rv0948c encoding the chorismate mutase enzyme.[1] Despite low sequence similarity (15%), both these proteins show chorismate mutase activity.[8] Rv1885c possesses an N-terminal signal sequence (33 amino acids) and is secreted out of mycobacterium. Extracellular Rv1885c is devoid of this signal sequence which indicates that the signal is cleaved-off at the time of secretion.[1] Although Rv1885c has chorismate mutase activity, it shares low sequence similarity with *Escherichia coli* (20%) or yeast (10%) chorismate mutase.[1,9] The crystal structure of Rv1885c (MtbCM) shows that it is a dimer, and belongs to AroQ class of protein.[8] MtbCM has a proline-rich (P-X-X-P) motif on the protein surface and resembles the eukaryotic SRC Homology 3 (SH3) binding domain. Interestingly, this SH3 binding domain is absent in non-secretory chorismate mutase (Rv0948c).

Secretory nature of MtbCM and a proline rich region on its surface that can participate in protein-protein interactions.[8] Indicate the probable role of MtbCM in host-pathogen interactions. Among the cytokines, interleukin-10 (IL-10) is important in establishing a successful *M. tuberculosis* infection in host,[10–13] whereas tumor necrosis factor-alpha (TNF-α) induces protective responses against the bacilli.[14] In the present study, MtbCM-mediated modulation of IL-10/TNF-α cytokine response and macrophage innate signaling is examined. It is

[1]Laboratory of Molecular Cell Biology, Centre for DNA Fingerprinting and Diagnostics (CDFD), Inner Ring Road, Uppal, Hyderabad, Telangana 500039, India
[2]Graduate Studies, Manipal Academy of Higher Education, Manipal, Karnataka 576104, India
[3]Graduate Studies, Regional Center for Biotechnology, Faridabad, Haryana (NCR Delhi) 121001, India
[4]Lead contact
*Correspondence: sangita@cdfd.org.in
https://doi.org/10.1016/j.isci.2024.111044

observed that MtbCM is a virulent factor helping the bacilli for a successful infection. MtbCM is secreted out and localizes to Golgi bodies in macrophages where it interacts with the AKAP9 protein (a scaffolding protein) through its SH3 binding domain. MtbCM-AKAP9 interaction inhibits phosphorylation of protein kinase C epsilon (PKCε) affecting the downstream MKP-1-p38 mitogen-activated protein kinase (MAPK) signaling axis resulting in upregulation of IL-10 but downregulation of TNF-α production. We have further shown that the SH3 binding domain of MtbCM is important for the mycobacterial virulence. This study highlights the important role of MtbCM and its SH3 binding domain in host-pathogen interaction and mycobacterial virulence which will help in designing novel and effective therapeutics to manage TB.

RESULTS

MtbCM is found to be secreted in the culture filtrate of Msmeg-MtbCM

Chorismate mutase is a secretory protein of *M. tuberculosis*.[15] Therefore, first, we examined whether Msmeg-MtbCM retained the ability to secrete MtbCM. MtbCM gene was expressed in a non-pathogenic *M. smegmatis* strain mc^2 155, which is widely used as a surrogate bacterium to characterize *M. tuberculosis* proteins[16] and was cultured in the Sauton's medium with kanamycin and hygromycin. When the absorbance at 600 nm reached about 0.8–1.0, the culture was harvested, and culture filtrate (CF) was examined for the presence of secreted MtbCM by Western blotting using anti-MtbCM Ab. The Ab was found to be specific to MtbCM as a single band corresponding to MtbCM was detected in the lysate prepared from Msmeg-MtbCM but not in the lysate prepared from Msmeg-pVV (Figure S1A). It was observed that Msmeg-MtbCM was able to secrete MtbCM in the CF (Figure S1B). GroEL1 protein was used as a control to eliminate the presence of bacterium or bacterial lysis in the culture filtrate. This indicates that MtbCM is secreted even when expressed in *M. smegmatis*. In the next experiment, RAW 264.7 macrophages were infected either with Msmeg-MtbCM or Msmeg-pVV at an MOI of 1:10. Cells were next harvested and observed for the presence of MtbCM following immunofluorescence technique using mouse anti-MtbCM Ab and Alexa Fluor 488–conjugated goat anti-mouse secondary Ab. Positive staining for MtbCM was observed in the cells infected with Msmeg-MtbCM but not with Msmeg-pVV (Figure S1C). This indicates that Msmeg-MtbCM was able to secrete MtbCM during infection in macrophages. Also, this result again indicates that anti-MtbCM Ab specifically recognizes the CM protein of *M. tuberculosis*. MtbCM is an important enzyme of the shikimate pathway. MtbCM belongs to the AroQ* class of enzymes and is required for aromatic amino acid biosynthesis.[15] Therefore, a growth curve assay was performed to observe the role of MtbCM in the growth kinetics of *M. smegmatis*. For this, 7H9 broth cultures were inoculated with an equal inoculum of either Msmeg-MtbCM or Msmeg-pVV, and absorbance at 600 nm was measured after every 4 h till the culture reaches saturation phase. Based on the absorbance values, growth rates were compared, and it was observed that ectopic expression of MtbCM did not impart any significant changes to the growth patterns of *M. smegmatis* (Figure S1D).

MtbCM upregulates IL-10 but downregulates TNF-α cytokine induction and provides better survival of the bacilli in macrophages

Next, we checked whether MtbCM acts as a virulence factor and enhances bacterial survival inside macrophages. The RAW 264.7 macrophages or the mouse peritoneal macrophages were infected with either Msmeg-pVV16 (control) or Msmeg-MtbCM, and intracellular survival of the bacilli was examined. We observed that with similar extent of phagocytosis (Figure 1A), as compared to Msmeg-pVV, Msmeg-MtbCM could survive better in RAW 264.7 macrophages (Figure 1B).

Cytokines are crucial in establishing mycobacterial infection and pathology.[17] For example, anti-inflammatory cytokine like IL-10 favors mycobacterial survival inside host cells, whereas pro-inflammatory cytokine like TNF-α provides immunity to the host against the bacilli.[18–20] Since MtbCM provides a survival advantage to the bacilli (Figure 1B), it was interesting to examine whether MtbCM modulates IL-10 and TNF-α induction profiles in macrophages. Therefore, RAW 264.7 macrophages were infected with either Msmeg-MtbCM or Msmeg-pVV at MOI of 1:10. Culture supernatants were harvested at 24 h and 48 h time points for measuring IL-10 and TNF-α cytokines. It was observed that RAW 264.7 macrophages infected with Msmeg-MtbCM produced higher levels of IL-10 but a lower amount of TNF-α as compared to macrophages infected with control Msmeg-pVV (Figures 1C and 1D). Similar results were observed in the Balb/c peritoneal macrophages infected with Msmeg-MtbCM versus Msmeg-pVV (Figures 1E–1G). Thus, MtbCM generates an anti-inflammatory milieu in macrophages which probably favors mycobacterial survival inside the host.

MtbCM manipulates IL-10 induction by regulating the PKCε-MKP-1-p38 MAPK signaling axis in macrophages

MAPKs are required for regulation of cytokine production. p38 MAPK is known to favor IL-10 production.[21,22] Since MtbCM upregulates IL-10 cytokine in macrophages, therefore, p38 MAPK activation was compared in RAW 264.7 macrophages infected with either Msmeg-MtbCM or Msmeg-pVV. It was observed that macrophages infected with Msmeg-MtbCM had a higher amount of phosphorylated p38 MAPK as compared to macrophages infected with Msmeg-pVV (Figures 2A and 2B). This indicates that MtbCM is involved in p38 MAPK activation.

To further confirm the direct role of p38 MAPK in MtbCM-mediated upregulation of IL-10, RAW 264.7 macrophages were next infected with Msmeg-MtbCM in the absence or presence of SB203580 (a pharmacological inhibitor of p38 MAPK). After 6 h of infection, cells were harvested and mRNA levels of IL-10 were measured in all the groups using real-time PCR (qPCR). It was observed that treatment of SB203580 downregulated IL-10 transcripts levels in macrophages infected with Msmeg-MtbCM when compared with macrophages infected with Msmeg-MtbCM without SB203580 (Figure 2C). Also, culture supernatants were collected after from RAW 264.7 macrophages infected with Msmeg-MtbCM in the absence or presence of SB203580 and IL-10 levels were quantified by EIA at both 24 h and 48 h time points. It was observed that macrophages pre-treated with SB203580 had a reduced level of IL-10 during infection with Msmeg-MtbCM as compared to

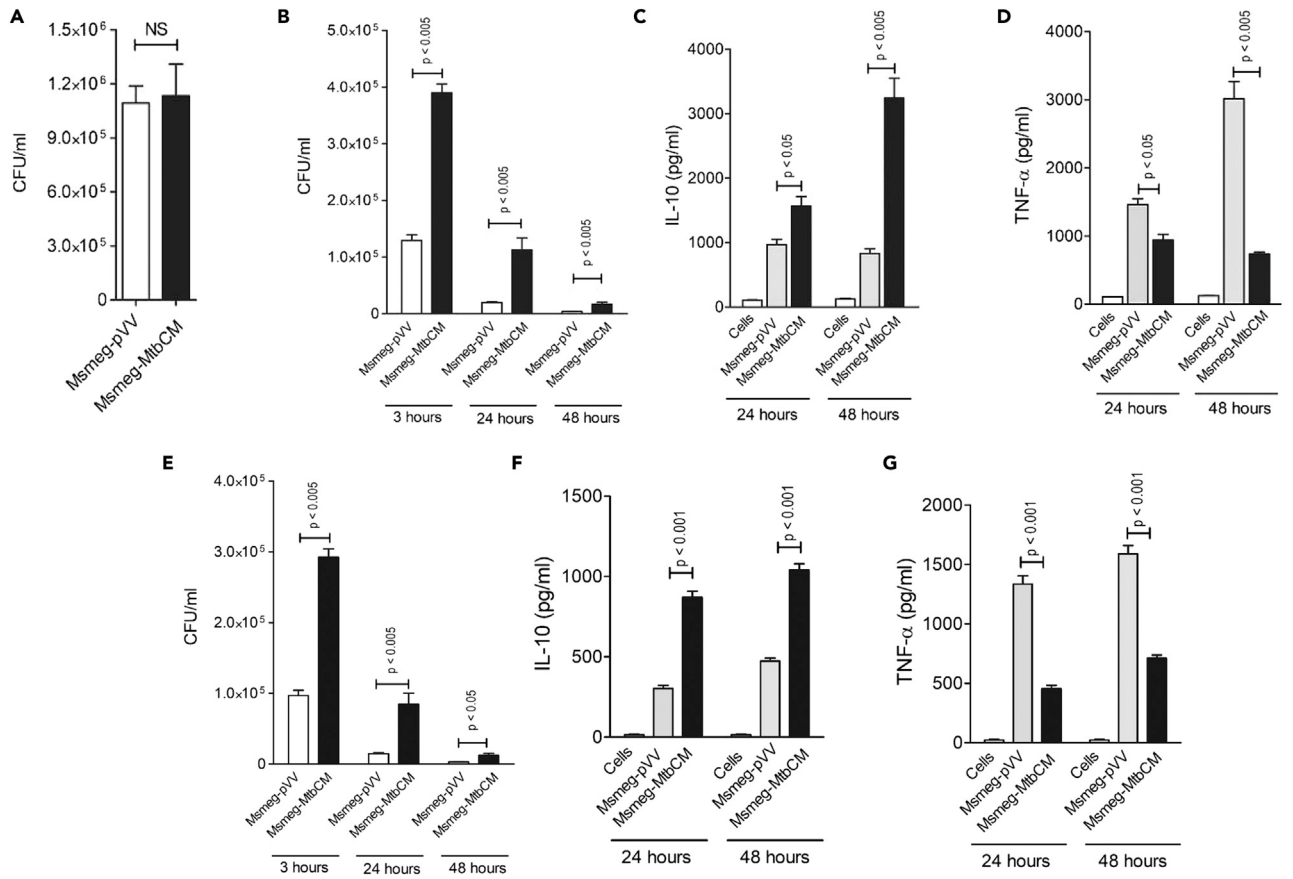

Figure 1. MtbCM renders survival advantage to *M. smegmatis* in macrophages and increases IL-10 but inhibits TNF-α production in macrophages

RAW 264.7 macrophages were infected with either Msmeg-pVV or Msmeg-MtbCM at MOI of 1:10. After 2 h, cells were washed to remove extracellular bacilli and were either harvested and lysed for CFU counts (A) or incubated for various time points and then lysed for determining CFU counts (B). The culture supernatants were harvested at 24 h and 48 h for measuring IL-10 (C) and TNF-α (D). In another set, peritoneal macrophages were infected with either Msmeg-MtbCM or Msmeg-pVV at MOI of 1:10 and after 3 h, 24 h and 48 h, cells were lysed for bacterial CFU counts (E) and culture supernatants were harvested for measuring IL-10 (F) and TNF-α (G) by two-site sandwich EIA respectively. Results are shown as Mean ± SEM of 3 independent experiments. Unpaired *t*-test was used to calculate the *p* values.

macrophages infected with Msmeg-MtbCM without SB203580 (Figure 2D). This indicates that MtbCM upregulates IL-10 directly by targeting the p38 MAPK signaling cascade.

The mitogen-activated protein kinase phosphatases (MKPs) are phosphatases that dephosphorylate MAP kinases and regulate their activity in cells. MKP-1 is known to dephosphorylate p38 MAPK and inhibit its activity.[22] Since Msmeg-MtbCM-infected macrophages showed increased activation of p38 MAPK, the level of MKP-1 was expected to be lower in macrophages infected with Msmeg-MtbCM than macrophages infected with Msmeg-pVV. When the levels of MKP-1 were measured in RAW 264.7 macrophages infected with Msmeg-MtbCM and compared with macrophages infected with Msmeg-pVV, it was observed that macrophages infected with Msmeg-MtbCM had reduced MKP-1 as compared to macrophages infected with Msmeg-pVV (Figures 3A and 3B).

MKP-1 stabilization in the macrophages is shown to be dependent upon IRAK3 localization.[22] It is observed that cytoplasmic translocation of IRAK3 from the nucleus is important for maintaining steady levels of MKP-1.[22] Since a reduced level of MKP-1 was observed in cells infected with Msmeg-MtbCM, the nuclear levels of IRAK3 were next investigated in macrophages during infection with Msmeg-MtbCM and compared with that of infection with Msmeg-pVV. Therefore, RAW 264.7 macrophages were infected with either Msmeg-MtbCM or Msmeg-pVV at an MOI of 1:10 and after 2 h of infection, cells were washed to remove extracellular bacteria and further incubated for 3 h and harvested for analysis of IRAK3 localization by immunofluorescence. It was observed that macrophages infected with Msmeg-MtbCM had nuclear enrichment of IRAK3 as compared to the macrophages infected with Msmeg-pVV (Figure 3C). This observation indicates that MtbCM inhibits IRAK3 function by restricting its cytoplasmic localization and thus affects MKP-1 stabilization.

Phosphorylation of PKCε is important for its kinase activity.[23] Our earlier reports have shown that the kinase activity of PKCε is essential for the nuclear export of IRAK3 to the cytoplasm.[22] We observed that infection with Msmeg-MtbCM resulted in poorer cytoplasmic migration of IRAK3 from nucleus, indicating the possibility of defective activation/phosphorylation of PKCε in macrophages infected with Msmeg-MtbCM.

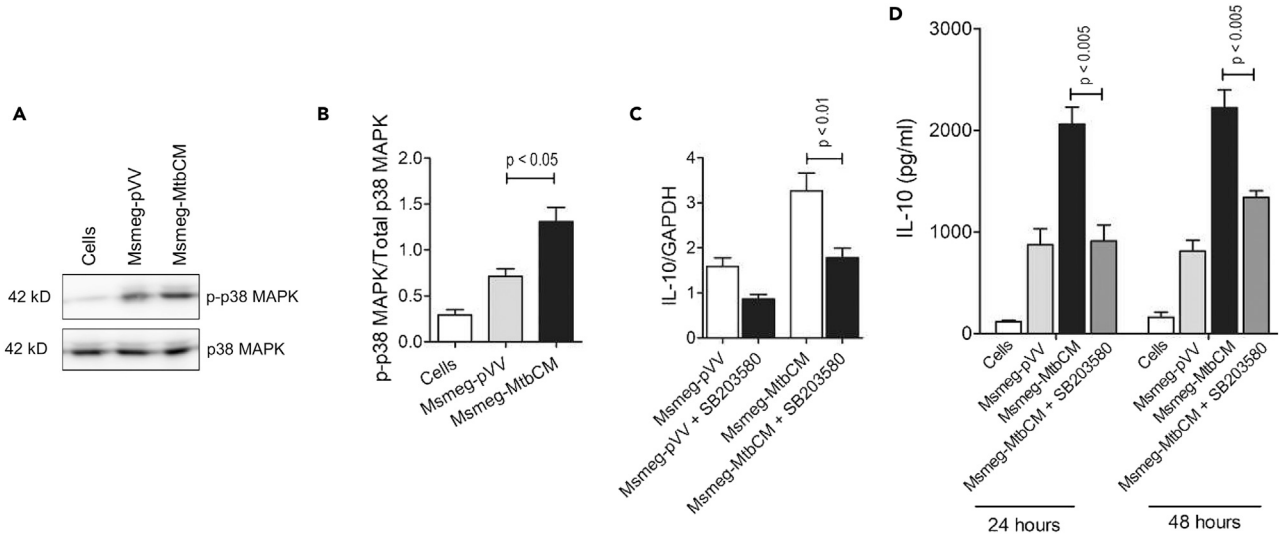

Figure 2. MtbCM increases p38 MAPK activation and targets p38 MAPK signaling cascade for upregulating IL-10 production in macrophages

RAW 264.7 macrophages were either treated with medium alone (cells) or infected with either Msmeg-pVV or Msmeg-MtbCM with MOI of 1:10. After 2 h of infection cells were washed to remove extracellular bacilli and further incubated for another 3 h. Next cells were harvested, and lysed to examine the levels of phosphorylated (p-p38 MAPK) and total p38 MAPK by Western blotting using anti-p-p38 MAPK and anti-p38 MAPK Ab respectively (A) and densitometric quantification of Western blots was carried out using ImageJ software (B). In another set of experiments RAW 264.7 macrophages were infected for 2 h with either Msmeg-pVV or Msmeg-MtbCM at MOI of 1:10 in the absence or presence of SB203580 (10 μM). Cells were either harvested after 3 h and used for cDNA synthesis and qPCR was performed to observe transcription levels of IL-10 with GAPDH as an internal control (C) or were cultured for 24 h and 48 h to detect IL-10 in the culture supernatants by EIA (D). Results shown are Mean ± SEM of 3 independent experiments. Unpaired *t*-test was used to calculate the *p* values.

Therefore, the phosphorylation status of PKCε was next examined in macrophages infected with Msmeg-MtbCM and was compared with macrophages infected with Msmeg-pVV. It was observed that macrophages infected with Msmeg-MtbCM had lesser phosphorylated PKCε levels as compared to macrophages infected with Msmeg-pVV (Figures 3D and 3E). This indicates that MtbCM inhibits phosphorylation/activation of PKCε resulted in its decreased kinase activity causing reduced export of IRAK3 from the nucleus to the cytoplasm. Taken these observations together, it can be concluded that MtbCM upregulates IL-10 production by targeting the PKCε-IRAK3-MKP-1-p38 MAPK signaling axis.

Next, it was checked whether MtbCM truly targets PKCε to regulate MKP-1-p38 MAPK signaling axis. Therefore, we used DCP-LA, a linoleic acid derivative, which is known to selectively and directly activates PKCε. In brief, RAW 264.7 macrophages were infected with Msmeg-pVV/Msmeg-MtbCM in the absence or presence of 100 nM DCP-LA and levels of phospho-p38 MAPK as well as MKP-1 were checked. Interestingly, we observed that RAW 264.7 macrophages infected with Msmeg-MtbCM had higher phospho-p38 MAPK as compared to RAW 264.7 macrophages infected with Msmeg-pVV which was expected (Figure 3F). However, in presence of the PKCε activator, DCP-LA, level of phospho-p38 MAPK was reduced in macrophages infected with Msmeg-MtbCM and is almost similar to the level observed in macrophages infected with Msmeg-pVV (Figure 3F). When the levels of MKP-1 in these groups were checked, it could be observed that MKP-1 expression level was poorer in Msmeg-MtbCM-infected RAW 264.7 macrophages as compared to Msmeg-pVV-infected macrophages, as expected (Figure 3G). However, the expression of inhibited-MKP-1 is re-increased after addition of DCP-LA (PKCε activator) in Msmeg-MtbCM-infected RAW 264.7 macrophages (Figure 3G). These data indicate that MtbCM targets the PKCε-MKP-1-p38 MAPK signaling axis.

Since, the importance of PKCε-MKP-1-p38 MAPK signaling axis in the regulation of IL-10 by MtbCM was established using RAW 264.7 macrophages, and since MtbCM also increased IL-10 in mouse-derived macrophages similar to RAW 264.7 macrophages, it was next checked whether MtbCM targets the PKCε-MKP-1-p38 MAPK signaling axis similarly in mouse-derived macrophages. Accordingly, peritoneal macrophages from Balb/c mice were infected with either Msmeg-MtbCM or Msmeg-pVV and the levels of phospho-PKCε-IRAK3-phospho-p38 MAPK was compared in these macrophages. It could be observed that as similar to RAW 264.7 macrophages, Msmeg-MtbCM reduced PKCε activation by inhibiting its phosphorylation in peritoneal macrophages also (Figure 4A) which resulted into decreased MKP-1 and higher p38 MAPK activation (Figures 4B and 4C) leading to higher IL-10 production (Figure 1F). This study highlights role of MtbCM in modulation of macrophage cytokine response by targeting the PKCε-MKP-1-p38 MAPK signaling axis.

AKAP9 is an interacting partner of MtbCM

Many eukaryotic kinases are characterized by the presence of the Src Homology 3 (SH3) domain which is important for controlling protein-protein interactions in several cell signaling cascades.[24] MtbCM is known to possess an SH3 binding domain near the C-terminal end.[8] Since MtbCM is secreted during infection, it might interact with one or more host protein(s) through its SH3 binding domain to influence the

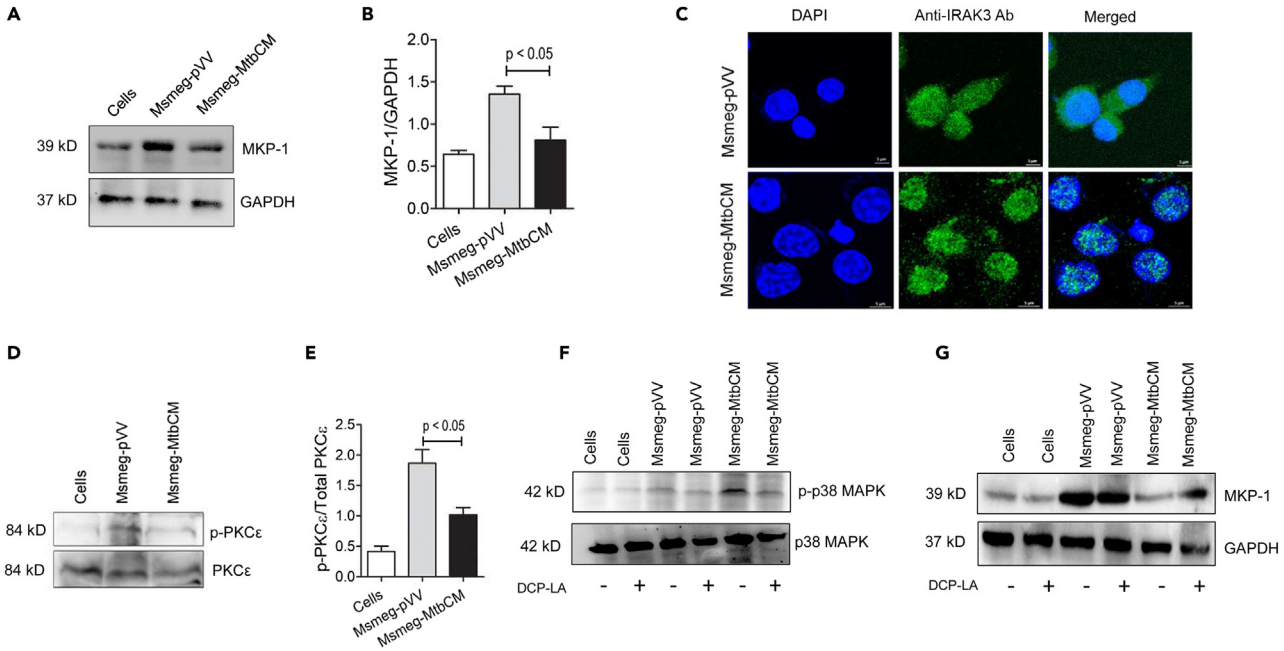

Figure 3. MtbCM affects the PKCε-IRAK3-MKP-1 signaling cascades in macrophages

RAW 264.7 macrophages were either treated with medium alone (cells) or infected with either Msmeg-pVV or Msmeg-MtbCM at MOI of 1:10. After 2 h of infection cells were washed to remove extracellular bacilli and incubated further for 3 h. Cells were lysed and the levels of MKP-1 were examined by Western blotting using anti-MKP-1 Ab (A). GAPDH was used as loading control and densitometric quantification of Western blots was performed using ImageJ software (B). Results shown are Mean ± SEM of 3 independent experiments. In another experiment, RAW 264.7 macrophages were infected with either Msmeg-pVV or Msmeg-MtbCM at 1:10 MOI. After 2 h of infection, cells were washed to remove extracellular bacilli and further incubated for another 3 h. Next cells were washed, fixed with 4% paraformaldehyde followed by permeabilization using 0.1% Triton X-100 and stained with anti-IRAK3 Ab at a dilution of 1:1000. Next, cells were washed and incubated with Alexa Flour-488 conjugated goat anti-rabbit secondary Ab at a dilution of 1:1000. After mounting with DAPI containing mounting medium, cells were observed under confocal microscope (C), (Scale bar: 5 μm). Results shown are representative of 3 different experiments. Also, lysates in Figure 3A were used to check the levels of phospho-PKCε and total PKCε by Western blotting using anti-phospho-PKCε Ab and total PKCε Ab respectively (D) and densitometric quantification of Western blot was performed using ImageJ software (E). Results shown are Mean ± SEM of 3 independent experiments. Unpaired *t*-test was used to calculate the *p* values for Figures 3B and 3E. In another experiment, RAW 264.7 macrophages were either treated with medium alone (cells) or infected with either Msmeg-pVV or Msmeg-MtbCM with MOI of 1:10 in the absence or presence of DCP-LA (100 nM). After 2 h of infection, cells were washed with 1X PBS to remove extracellular bacilli and incubated for another 2 h. Cells were harvested and protein lysates were prepared and analyzed for phosphorylated p38 MAPK (p-p38 MAPK) and total p38 MAPK (F) as well as MKP-1 (G) protein levels by Western blotting using specific antibodies. GAPDH was used as a loading control. Results shown are representative of 3 different experiments.

downstream PKCε signaling cascades. To further gain insights into the mechanism of action of MtbCM in regulating PKCε signaling, a proteomics-based identification of MtbCM-interacting partner(s) was performed. Therefore, metal affinity chromatography was used to purify recombinant MtbCM, and eluted fractions were run on 10% SDS-PAGE gel followed by Coomassie Brilliant Blue (R250) staining. A purified fraction of recombinant MtbCM was observed at ~25 kDa (Figure S2A). Next, bacterial lipopolysaccharide (LPS)-treated RAW 264.7 macrophages were harvested and lysed and cell lysate was incubated with TALON beads containing MtbCM for 12 h–14 h at 4°C. Beads were then harvested and the bound proteins were resolved by 10% SDS-PAGE. TALON beads alone (without MtbCM) incubated with the cell lysate were used as control. Next, silver staining was performed on the SDS-PAGE gel. Specific bands observed in the presence of MtbCM were cut and subjected to further processing for MS/MS analysis using MALDI-TOF. The data were analyzed using MASCOT DATA SEARCH software and a protein A-kinase anchor protein-9 (AKAP9) was identified as the interacting partner of MtbCM (Figures S2B and S2C).

MtbCM binds with AKAP9 during infection and inhibits AKAP9-PKCε interaction

Based on the mass spectrometry analysis, AKAP9 was identified as the interacting protein of MtbCM. To confirm the interaction of MtbCM with AKAP9 during infection conditions, RAW 264.7 macrophages were infected with Msmeg-MtbCM. The cells were harvested and AKAP9 was immunoprecipitated using rabbit anti-AKAP9 Ab. Rabbit IgG was used as an isotype control. The pulled-down products were resolved on SDS-PAGE gel followed by Western blotting using anti-MtbCM Ab. It was observed that MtbCM was co-immunoprecipitated with AKAP9 in macrophages infected with Msmeg-MtbCM (Figure 5A).

AKAP9 is a Golgi localized, scaffolding protein that assembles and facilitates phosphorylation of several protein kinases.[25] It has been found that the activation loop site of PKC is phosphorylated by phosphoinositide-dependent kinase 1 (PDK1)[26] and it has been shown that PDK1 is important for the PKCε phosphorylation at Ser(729).[27] It has been reported that PKC scaffolding by AKAPs can have a profound

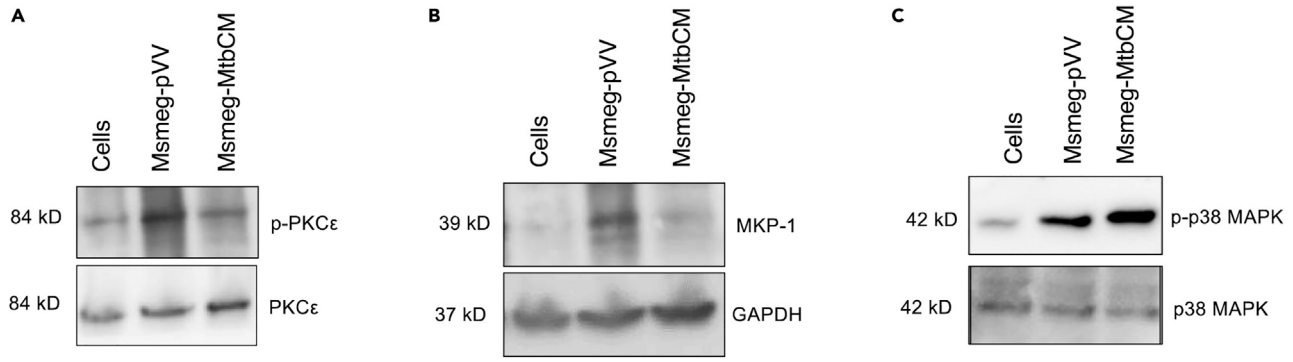

Figure 4. MtbCM targets the PKCε-MKP-1-p38 MAPK signaling axis in infected peritoneal macrophages

Peritoneal macrophages isolated from Balb/c mice were either treated with medium alone (cells) or infected with either Msmeg-pVV or Msmeg-MtbCM at MOI of 1:10. After 2 h of infection, cells were washed with 1X PBS to remove extracellular bacilli and were further incubated for 3 h. Cells were lysed and protein levels of phospho-PKCε and total PKCε (A), as well as MKP-1 (B) and phospho-p38 MAPK and total p38 MAPK (C) were assessed by Western blotting using specific Abs. GAPDH was used as loading control for (B). Results shown are representative of 3 different experiments.

effect on tuning the PKC activity.[28] Interestingly, AKAP9-PKCε interaction is shown to be essential for the regulation of PKCε phosphorylation and activity.[29] Since Msmeg-MtbCM-infected macrophages showed downregulation of PKCε phosphorylation and as AKAP9-PKCε interaction is essential for regulation of PKCε phosphorylation, we speculated that, interaction of MtbCM with AKAP9 could result in inhibition of AKAP9-PKCε complex formation which subsequently causes reduction in PKCε phosphorylation. To confirm this hypothesis, RAW 264.7 macrophages were infected with Msmeg-MtbCM or Msmeg-pVV. Cells were harvested and AKAP9 was immunoprecipitated using anti-AKAP9 Ab. The pulled-down products were resolved on SDS-PAGE followed by Western blotting using anti-PKCε Ab. In the presence of MtbCM, weaker AKAP9-PKCε interaction was observed (Figure 5B) which probably resulted in reduced PKCε phosphorylation as observed in Figure 3D.

MtbCM localizes to Golgi body

AKAP9 is a Golgi resident protein and MtbCM was found to interact with AKAP9. Since MtbCM was shown to be secreted during infection of macrophages with Msmeg-MtbCM, it is possible that MtbCM is migrated to Golgi where it interacts with AKAP9. Therefore, it was investigated whether MtbCM is localized in Golgi. Accordingly, HEK-293T cells were co-transfected with pEGFP-MtbCM and mCherry-TGOLN2 plasmids (a marker for the trans-Golgi network). HEK-293T cells co-transfected with backbone vector (pEGFP) and mCherry-TGOLN2 were used as control group. After 24 h of transfection, cells were harvested, fixed, and observed under confocal microscope. It was found that pEGFP-MtbCM was co-localized with mCherry-TGOLN2 (Figures 6A and 6B). This observation indicates that MtbCM gets localized to the Golgi body.

To further confirm the Golgi localization of MtbCM during infection, RAW 264.7 macrophages were infected with either Msmeg-MtbCM or Msmeg-pVV. After 2 h, cells were washed to remove extracellular bacilli and incubated further for 3 h. Golgi fractions were isolated and the presence of MtbCM in the Golgi fraction was examined by Western blotting using anti-MtbCM Ab and MtbCM was found to be present in the Golgi fraction of macrophages infected with Msmeg-MtbCM but not in that infected with Msmeg-pVV (Figure 6C). Also, it was possible to pull-down MtbCM along with its interacting partner AKAP9 from the enriched Golgi fraction of Msmeg-MtbCM-infected cells. These observations confirm that during infection, MtbCM migrates to Golgi where it interacts with AKAP9 (Figure 6D).

SH3 binding domain of MtbCM is important for the regulation of IL-10 production and survival of bacilli inside macrophages

In the earlier section, it has been shown that MtbCM is localized to Golgi where it interacts with AKAP9. Since, MtbCM contains an SH3 binding domain,[8] it was next investigated whether MtbCM interacts with AKAP9 through its SH3 binding domain. Therefore, all the four proline residues in the SH3 binding domain (PPEPP motif) of MtbCM were replaced with serine residues by site-directed mutagenesis (Figure S3A). The mutant MtbCM (MtbCM-PS4) was cloned in the pVV16 vector and expressed in *M. smegmatis* (Msmeg-MtbCM-PS4) and expression of the mutant protein was confirmed by Western blotting using anti-MtbCM Ab (Figure S3B). Next, it was examined whether the mutant protein (MtbCM-PS4) was secreted during infection of macrophages with Msmeg-MtbCM-PS4. The immunofluorescence microscopy indicated the presence of MtbCM-PS4 protein in macrophages infected with Msmeg-MtbCM-PS4 but not with Msmeg-pVV suggesting that mutation in the SH3 binding domain of MtbCM did not affect the secretion of the protein by the bacilli during infection of macrophages (Figure S3C).

Since MtbCM is a functional chorismate mutase enzyme,[1] therefore, the enzymatic activity of MtbCM-PS4 was compared with MtbCM. Accordingly, lysates were prepared from Msmeg-pVV, Msmeg-MtbCM, and Msmeg-MtbCM-PS4, and chorismate mutase activity was measured. It was observed that both Msmeg-MtbCM and Msmeg-MtbCM-PS4 had significantly higher chorismate mutase activity as

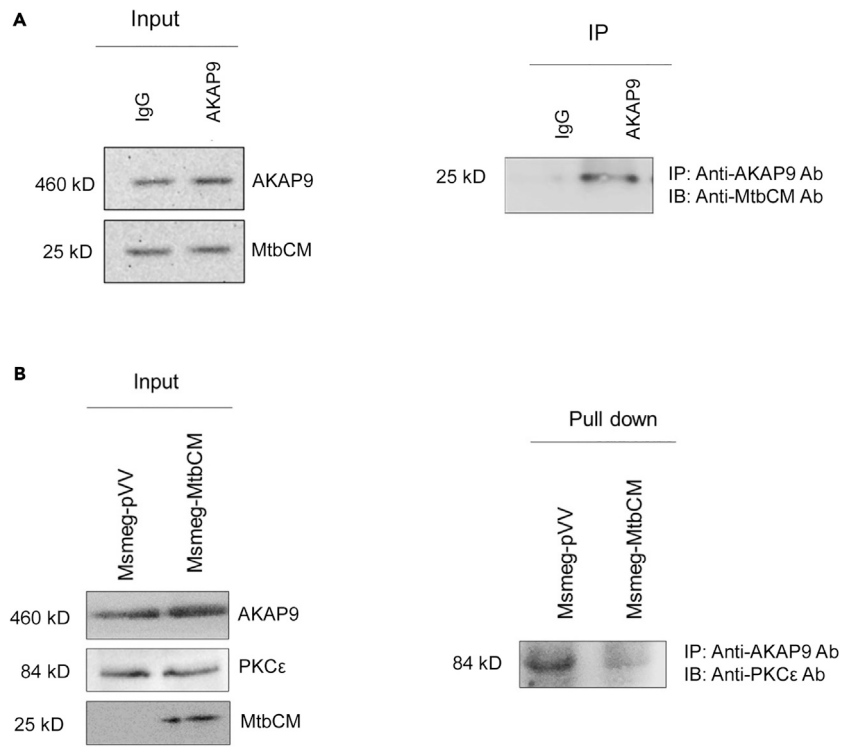

Figure 5. MtbCM interacts with AKAP9 and inhibits AKAP9-PKCε interaction in infected macrophages

RAW 264.7 macrophages were infected with Msmeg-MtbCM at MOI of 1:50. After 5 h of infection cells were harvested, lysed and AKAP9 was immunoprecipitated (IP) using anti-AKAP9 Ab. The pull-down product was immunoblotted (IB) with anti-MtbCM Ab to detect MtbCM and total levels of AKAP9 and MtbCM in both the groups were shown as input controls (A). Results shown are representative of 3 different experiments. In another experiment, RAW 264.7 macrophages were infected with Msmeg-MtbCM at MOI of 1:50. After 5 h, cells were harvested, lysed and AKAP9 was immunoprecipitated (IP) using anti-AKAP9 Ab. The pull-down product was immunoblotted (IB) using anti-PKCε Ab to detect PKCε (B). Total levels of AKAP9, PKCε and MtbCM in both the groups were shown as input controls. Results shown are representative of 3 different experiments.

compared to Msmeg-pVV (Figure S4). Interestingly, lysates prepared from Msmeg-MtbCM and Msmeg-MtbCM-PS4 had comparable chorismate mutase activity (Figure S4) indicating that mutation in the SH3 binding domain (**PPEPP** to **SSESS**) did not affect the enzymatic activity of MtbCM.

To examine the role of the SH3 binding domain of MtbCM in the MtbCM-AKAP9 interaction, RAW 264.7 macrophages were infected with either Msmeg-MtbCM or Msmeg-MtbCM-PS4 for 2 h. The extracellular bacteria were removed and cells were incubated for another 3 h. Next, cells were harvested and AKAP9 was immunoprecipitated using anti-AKAP9 Ab. The immune complex was subjected to Western blotting using either anti-MtbCM Ab or anti-PKCε Ab. Though a stronger interaction was observed between MtbCM and AKAP9, which was expected, a poorer interaction was observed between AKAP9 and MtbCM-PS4 indicating that the SH3 binding domain of MtbCM plays a crucial role in its interaction with AKAP9 (Figure 7A). As expected, higher AKAP9-PKCε interaction was observed in macrophages infected with Msmge-MtbCM-PS4 as compared to macrophages infected with Msmeg-MtbCM (Figure 7A).

It has been observed that MtbCM interferes with PKCε-p38 MAPK signaling axis and IL-10 induction due to its direct interaction with AKAP9 which is mediated through the SH3 binding motif of MtbCM. Thus, it can be speculated that the SH3 binding domain of MtbCM is responsible for the regulation PKCε-p38 MAPK signaling cascades and the consequent production of IL-10. Therefore, PKCε and p38 MAPK phosphorylation levels were compared in macrophages infected with Msmeg-MtbCM versus Msmeg-MtbCM-PS4. It was observed that macrophages infected with Msmeg-MtbCM-PS4 had increased levels of PKCε phosphorylation (Figure 7B) but decreased p38 MAPK phosphorylation (Figure 7C) when compared with macrophages infected with Msmeg-MtbCM and comparable to the levels observed in Msmeg-pVV. Thus, MtbCM-PS4 that fails to interact with AKAP9 favors a more robust AKAP9-PKCε interaction to increase phosphorylation of PKCε which subsequently results in decreased p38 MAPK phosphorylation.

Since the PKCε-p38 MAPK signaling axis is critical for IL-10 production in macrophages,[22] the levels of IL-10 production were compared in RAW 264.7 macrophages infected with Msmeg-MtbCM versus Msmeg-MtbCM-PS4. Accordingly, RAW 264.7 macrophages were infected with Msmeg-pVV or Msmeg-MtbCM or Msmeg-MtbCM-PS4 with an MOI of 1:10. Uninfected cells were used as control. Levels of IL-10 cytokine were measured in culture supernatants at 24 h and 48 h time points. It was observed that Msmeg-MtbCM-PS4-infected cells had lower levels of IL-10 as compared to Msmeg-MtbCM-infected macrophages and comparable to the levels observed in Msmeg-pVV (Figure 7D). These observations further indicate that MtbCM modulates IL-10 production by its interaction with AKAP9 through the SH3 binding domain.

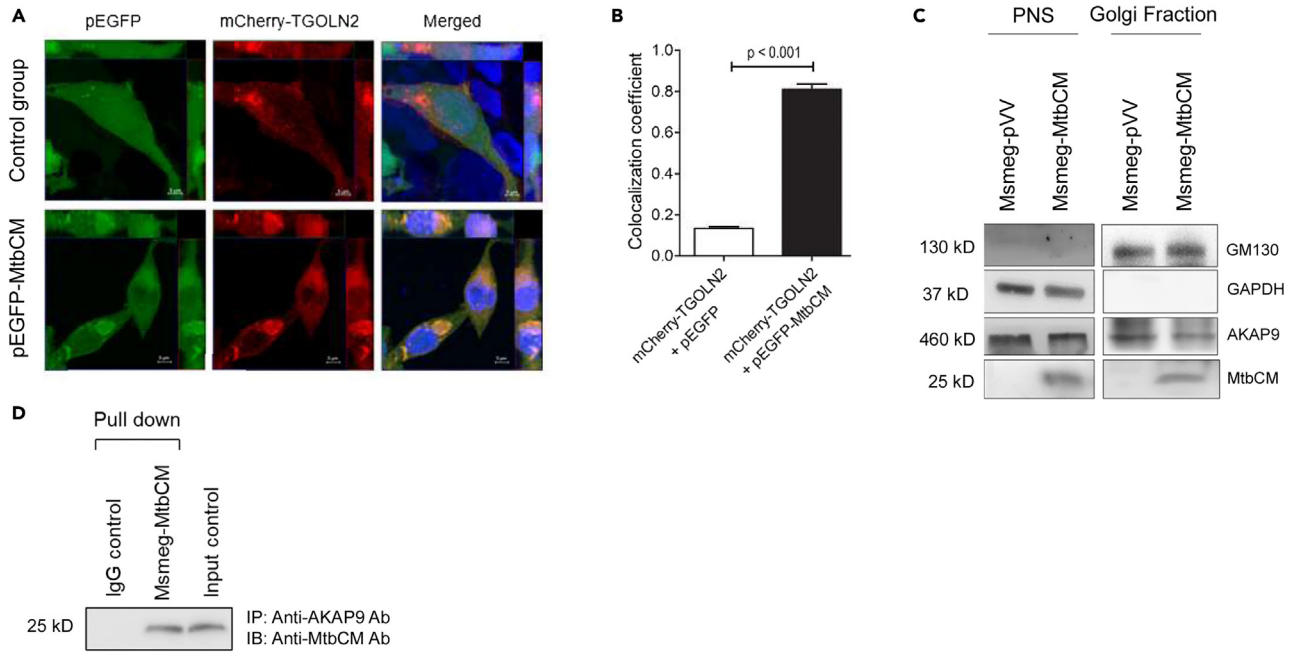

Figure 6. MtbCM localizes to Golgi network where it interacts with AKAP9

HEK-293T cells were transiently co-transfected with either pEGFP-MtbCM or pEGFP along with mCherry-TGOLN2. Cells were fixed using 4% formaldehyde and were observed under confocal microscope. DAPI was used to stain the nucleus (blue), (Scale bar: 1μm) (A). Colocalization coefficient was calculated using ZEN 2 (blue edition) software and was shown as Mean ± SEM from 50 cells of 3 independent experiments (B). In another experiment, RAW 264.7 macrophages were infected with either Msmeg-pVV or Msmeg-MtbCM at MOI of 1:50. Next, Golgi fractions were isolated. About 25 μg of PNS and Golgi fractions were resolved on SDS-PAGE and immunoblotted using either anti-AKAP9 Ab or anti-MtbCM Ab to show the presence of AKAP9 and MtbCM in the Golgi fraction (C). GAPDH was used as a negative control and GM130 was used as a Golgi marker. Next, AKAP9 was immunoprecipitated from cell lysates prepared from macrophages infected with Msmeg-pVV/Msmeg-MtbCM using anti-AKAP9 Ab and the pull-down product was immunoblotted using anti-MtbCM Ab to confirm AKAP9-MtbCM interaction (D). Results are representative of 3 independent experiments.

To understand whether the SH3 binding domain of MtbCM plays a role in dictating the survival of the bacilli in macrophages, RAW 264.7 macrophages were infected with either Msmeg-pVV or Msmeg-MtbCM or Msmeg-MtbCM-PS4 at MOI of 1:10 and intracellular survival of mycobacteria was monitored. It was observed that as compared to Msmeg-pVV, survival rate of Msmeg-MtbCM was significantly higher in macrophages at all the time points tested (3 h, 24 h, and 48 h). However, the survival rate of Msmeg-MtbCM-PS4 was poorer with a comparable CFU count with Msmeg-pVV (Figure 7E). These observations indicate that the SH3 binding domain of MtbCM is important for its virulence.

Next, the importance of AKAP9 in the regulation of IL-10 by MtbCM was examined by silencing AKAP9 in RAW 264.7 macrophages using AKAP9-specific siRNA and more than 90% inhibition of AKAP9 was observed in this macrophage receiving AKAP9 siRNA (AKAP-KD) as compared to RAW 264.7 macrophages receiving control siRNA (AKAP-CT) (Figure 7F). An increased induction of IL-10 was observed in AKAP-CT infected with Msmeg-MtbCM when compared with IL-10 level induced in AKAP-CT infected with either Msmeg-pVV or Msmeg-MtbCM-PS4, which was expected (Figure 7G). Interestingly, an increased IL-10 induction was observed in AKAP-KD infected with either Msmeg-pVV or Msmeg-MtbCM-PS4 when compared with AKAP-CT infected with either Msmeg-pVV or Msmeg-MtbCM-PS4 and the level of IL-10 in AKAP-KD infected with Msmeg-pVV/Msmeg-MtbCM-PS4 was almost equal to the level of IL-10 induced in AKAP-CT infected with Msmeg-MtbCM (Figure 7G). Expectedly not much difference in IL-10 level was observed in AKAP-CT versus AKAP-KD, both infected with Msmeg-MtbCM which was expected (Figure 7G). These data indicate that IL-10 signaling in Msmeg-pVV/Msmeg-MtbCM-PS4-infected RAW 264.7 macrophages was regulated upstream by AKAP9 and MtbCM by directly interacting with AKAP9 through its SH3 binding domain could manipulate APAP9 signaling resulting in increased IL-10 production during infection of macrophages with Msmeg-MtbCM.

To confirm the role of MtbCM in the virulence of mycobacteria, we next infected Balb/c mice with 5×10^7 CFU of either Msmeg-pVV or Msmeg-MtbCM or Msmeg-MtbCM-PS4. After day 3, day 5, and day 15, mice were sacrificed and the liver, lung, and spleen tissues were harvested for counting bacterial burden. We observed higher CFU counts of Msmeg-MtbCM in all the organs at all the time points as compared to Msmeg-pVV or Msmeg-MtbCM-PS4 (Figures 8A–8D). This indicates that in the mouse model of infection, MtbCM provides a survival advantage to *M. smegmatis* and the SH3 domain of the MtbCM is important for its virulence. When we examined the levels of IL-10 in the lysates prepared from lung and spleen at day 7, it was observed that IL-10 levels were higher in both lung and spleen of mice infected with Msmeg-MtbCM as compared to mice infected with Msmeg-pVV or Msmeg-MtbCM-PS4 (Figures 8E and 8F). These studies indicate that the SH3 domain of MtbCM plays an important role in activation of IL-10 and mycobacterial virulence during infection in mice.

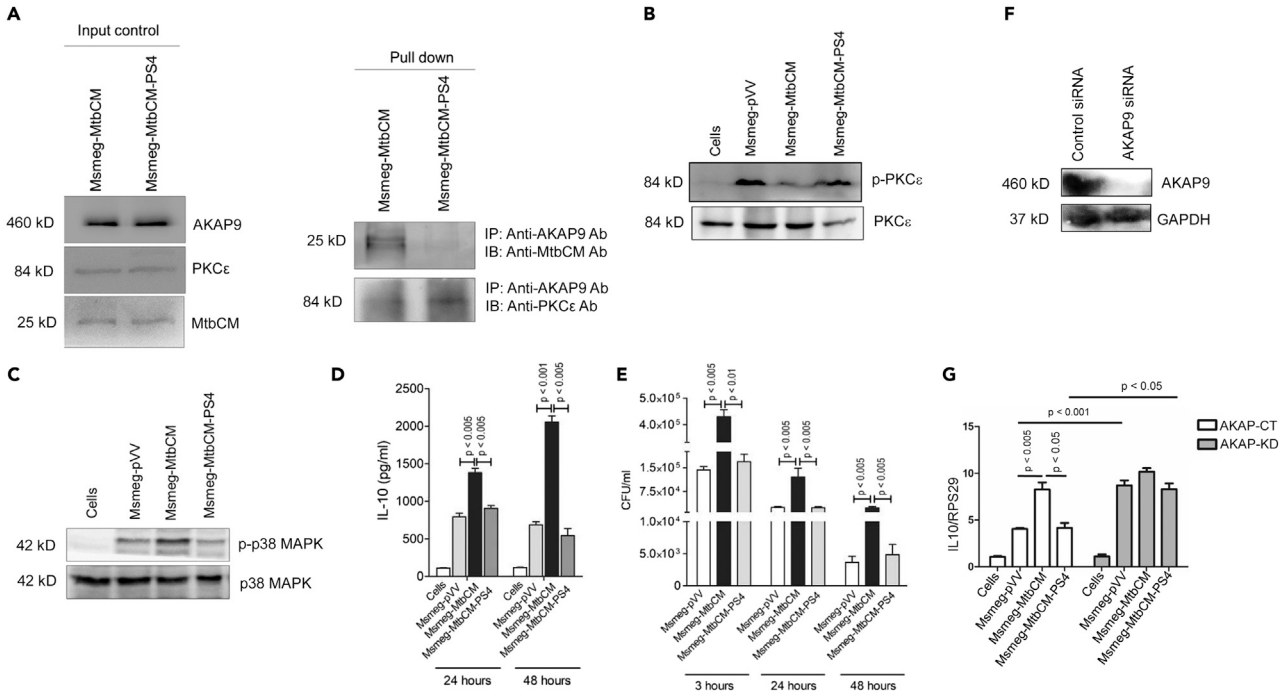

Figure 7. SH3 binding domain of MtbCM is important for its interaction with AKAP9 and IL-10 signaling and survival of bacilli inside macrophages

RAW 264.7 macrophages were infected with either Msmeg-MtbCM or Msmeg-MtbCM-PS4 with MOI of 1:50. After 5 h, cells were harvested, lysed and AKAP9 was immunoprecipitated (IP) with anti-AKAP9 Ab and the pull-down product was immunoblotted (IB) with either anti-MtbCM Ab or anti-PKCε Ab (A). The results are representative of 3 independent experiments.

(B and C) Again, RAW 264.7 macrophages were left uninfected or infected with either Msmeg-pVV or Msmeg-MtbCM or Msmeg-MtbCM-PS4 at MOI 1:10. After 2 h of infection, cells were washed to remove extracellular bacilli and further incubated for another 3 h. Next cells were harvested and lysates were analyzed either for phosphorylated PKCε (*p*-PKCε) and total PKCε (B) or for phosphorylated p38 MAPK (p-p38 MAPK) and total p38 MAPK (C) by Western blotting using specific combinations of primary and secondary antibodies. In another experiment, RAW 264.7 macrophages were infected with either Msmeg-pVV or Msmeg-MtbCM or Msmeg-MtbCM-PS4 at MOI of 1:10. After 24 h and 48 h, culture supernatants were collected for measuring IL-10 by two-site sandwich EIA (D). Results were shown as Mean ± SEM of 3 independent experiments. Also, RAW 264.7 macrophages were infected with either Msmeg-pVV or Msmeg-MtbCM or Msmeg-MtbCM-PS4 at MOI of 1:10. After 2 h of infection, cells were washed to remove extracellular bacilli and incubated for various time points, lysed and plated for CFU counts (E). In another experiment, RAW 264.7 macrophages were transfected with either control siRNA (AKAP-CT) or AKAP9 siRNA (AKAP-KD). After 24 h, cells were harvested, lysed and inhibition of AKAP9 protein levels was checked by Western blotting using anti-AKAP9 antibody and GAPDH was used as loading control (F). Next, AKAP-CT or AKAP-KD RAW 264.7 macrophages were infected with either Msmeg-pVV or Msmeg-MtbCM or Msmeg-MtbCM-PS4 with MOI of 1:10 or treated with medium alone (cells). After 2 h of infection, cells were washed to remove the extracellular bacilli and incubated further for 6 h. Cells were harvested and used for RNA isolation and cDNA synthesis and then qPCR was performed to find the mRNA levels of IL-10 (G). RPS29 transcript level was used as internal control. Results were shown as Mean ± SEM of 3 independent experiments. Unpaired *t*-test was used to calculate the *p* values.

DISCUSSION

M. tuberculosis has infected more than 10 million people in 2023[30] and is the leading cause of deaths from a single infectious agent. *M. tuberculosis* possesses a battery of virulence factors to modulate host immune responses to favor its intracellular survival and establishment of the disease. The complete genome sequence of *M. tuberculosis* has revealed several known as well as putative virulent factors, and many of them are secretory in nature.[31] The secretory proteins of *M. tuberculosis* are shown to inhibit the protective host immune responses by blocking one or more cellular processes.[32–36]

Cytokine signaling plays a crucial role in dictating the host innate and subsequent adaptive immune responses required in clearing the invading pathogen. Several reports have shown that *M. tuberculosis* modulates various cytokine levels in infected macrophages to enhance its intracellular survival and establishment of infection.[36,37] IL-10 is one of the cytokines induced by macrophages infected with *M. tuberculosis*. IL-10 predominantly polarizes the T-helper (Th) cells to be skewed toward the Th2-type which is known to favor intracellular survival of mycobacteria.[11,38,39] Also, IL-10 inhibits pro-inflammatory Th1 cytokines like IFN-γ,[40,41] IL-12 and TNF-α[40,42] to suppress the Th1-type immune responses which is important for host's protective immunity against the bacilli.[43] *M. tuberculosis* is known to employ various strategies to modulate macrophage signaling cascades to skew Th polarity toward the Th2-type.[44–47] It has been found that mycobacterial cell wall components can inhibit transcriptional responses to IFN-γ[48,49] or reduce its production.[50] On the other hand, *M. tuberculosis* can induce IL-10 cytokine production through activation of TLR2-signaling pathway through ligands like Rv1265[51] or *M. tuberculosis* heat shock protein 60[52] or PPE18[11] which presumably enhances intracellular survival of bacilli in mice infection model.[12,38] Interestingly, anti-PPD T cell response

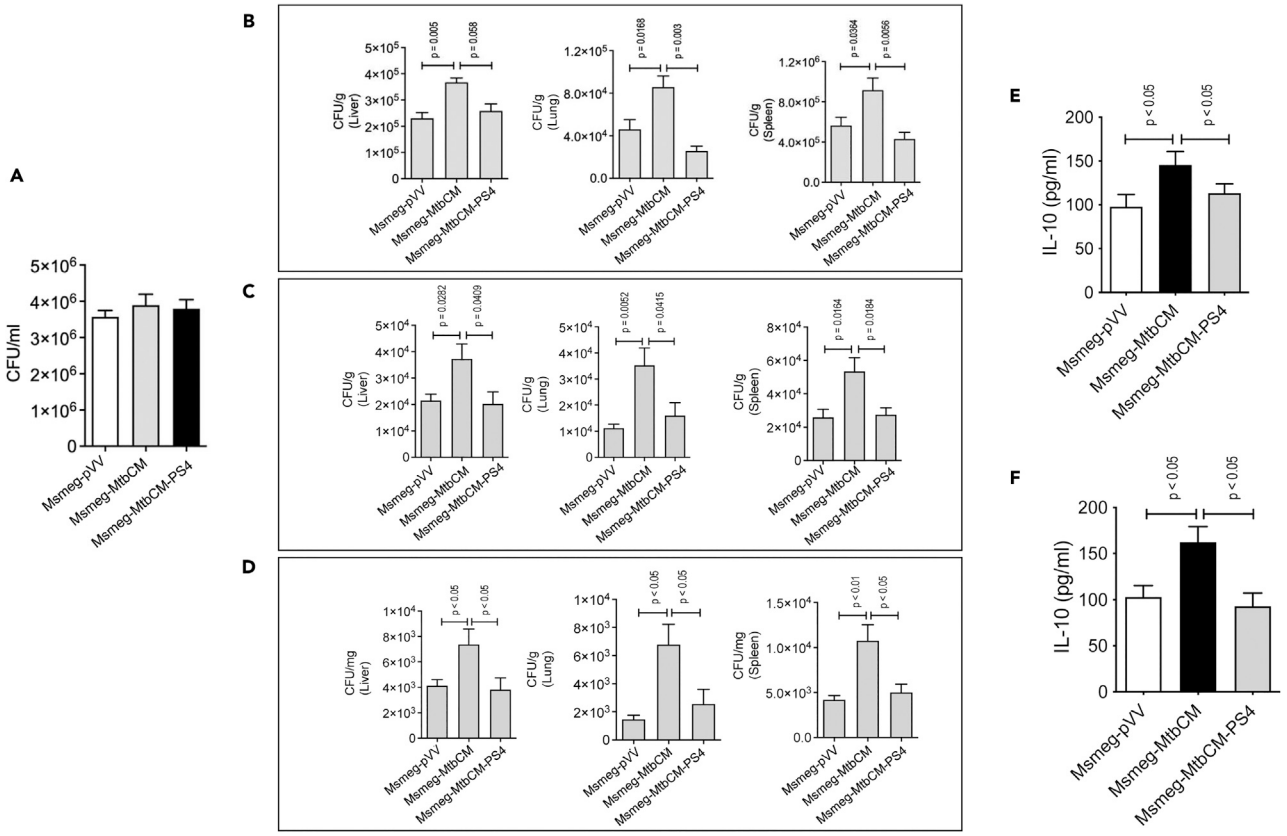

Figure 8. MtbCM confers the survival advantage and activates IL-10 production in mice

Balb/c mice ($n = 8$) were infected intravenously with equal number (5×10^7) of either Msmeg-pVV or Msmeg-MtbCM or Msmeg-MtbCM-PS4 (A), and sacrificed after 3 (B), 5 (C) and 15 (D) days post-infection for determination of CFU counts in liver, lung and spleen. Also, IL-10 was measured in the tissue lysates of lung (E) and spleen (F) by two-site sandwich EIA. The Data represent mean ± SEM of 8 mice per group for each time point. Unpaired *t*-test was used to calculate the *p* values.

is shown to be skewed toward the Th2-type in active TB patients further establishing a link between IL-10/Th2 and active TB infection.[47,53,54] Thus, it appears that several Mtb factors are involved in manipulating macrophage signaling cascades to activate IL-10 production and targeting these proteins are crucial to implement appropriate therapeutics to control TB infection. It is pertinent to note that blocking the Th2 component is more important than enhancing the existing Th1 response.[44,45] In this context, it is important to identify the crucial virulent factor(s) and the mechanism(s) that enhances IL-10/Th2 response during mycobacterial infection.

In the present study, we demonstrate that the secretory chorismate mutase (Rv1885c) can upregulate IL-10 production in macrophages. It has been shown that during infection, the secreted MtbCM localizes to the Golgi bodies of macrophages where it interacts with AKAP9 protein which is a scaffolding protein and facilitates phosphorylation of protein kinases[55] including PKCε.[29] AKAP9-PKCε interaction is required for phosphorylation of PKCε and hence its activation.[27] PKCε binds to the AKAP9 to get phosphorylated by PDK1.[26] Herein, we show that in the presence of MtbCM, AKAP9-PKCε interaction was inhibited resulting in poorer PKCε phosphorylation. Earlier, we demonstrated that PKCε-IRAK3-p38 MAPK signaling axis is critical for induction of IL-10 cytokine in macrophages.[22] MtbCM-mediated suppression of PKCε phosphorylation/activation restricts its ability to regulate IRAK3 export from the nucleus to the cytoplasm resulting in downregulation of MKP-1 stabilization. MKP-1 is a phosphatase that maintains the phosphorylation status of p38 MAPK in the cells[22] and IL-10 expression in macrophages is directly linked to phosphorylation status of p38 MAPK.[56] MtbCM-mediated activation of p38 MAPK resulted in higher IL-10 production which might be one of the reasons for enhanced intracellular survival of the bacilli.[12,13,39] Similarly, PPE18 protein of Mtb also targets the PKCε-IRAK3-p38 MAPK signaling to activate IL-10 production, however, PPE18 targets the TLR2 11–15 leucine rich repeat (LRR) domain unlike MtbCM that targets AKAP9. Thus, Mtb uses multipronged strategies to activate IL-10 cytokine, once during infection by manipulating TLR2-triggered signaling engaging PPE18 and other proteins and also later by targeting the AKAP9-signaling after infection through secretory MtbCM protein. Thus, it appears that *M. tuberculosis* spatially and temporally manipulates the macrophage signaling to induce IL-10 through several effector proteins to successfully survive and persist inside macrophages.

In a structure-based study, it was found that MtbCM possesses SH3 binding domain at C-terminus.[8] The presence of such motifs are common features of many eukaryotic kinases and are important for cellular signaling and communication.[24] The present study highlights the role of the SH3 domain of MtbCM in the modulation of macrophage effector function and mycobacterial virulence. It was shown that the MtbCM

interacts with AKAP9 via its SH3 binding domain and modulates IL-10 production. Mutation in the SH3 binding domain of MtbCM (MtbCM-PS4) resulted in reduced IL-10 production and poor intracellular survival of the bacteria. This indicates that the SH3 binding domain of MtbCM has a prominent role in IL-10 signaling and mycobacterial virulence.

Shikimate pathway is conspicuously absent in mammals and chorismate mutase, one of the seven enzymes in this pathway is essential for the synthesis of aromatic amino acids in *M. tuberculosis*. This attribute makes the shikimate pathways and MtbCM an attractive drug target for the treatment of TB. The present study has identified that in addition to its chorismate mutase enzyme activity, MtbCM is also important for mycobacterial virulence. This additional information might help in the development of more specific drugs against MtbCM to tackle tuberculosis. To the best of our knowledge, we demonstrate that SH3 binding domain of a Mtb protein (MtbCM) modulates host immune responses skewing the response toward the Th2-type and regulates mycobacterial virulence.

Limitations of the study

Our studies have a few limitations. The entire study has been done using *Mycobacterium smegmatis* expressing chorismate mutase protein of *M. tuberculosis* (MtbCM). However, it is very much needed to carry out this study using wild-type versus MtbCM knock-out *M. tuberculosis* in macrophage and in mice model to consistently prove a role of MtbCM in mycobacterial virulence by favoring a Th2/IL-10-dominated immune environment. Future research is required to carry out through RNA-seq studies to investigate other pathways that might be modulated by MtbCM to influence various macrophage innate-effector functions in addition to modulation of IL-10/TNF-α cytokine signaling axis. Another limitation in this study is that we found that the SH3-binding domain of MtbCM contributes to mycobacterial virulence, therefore, studies need to be carried out focusing SH3-binding domain of MtbCM as a therapeutic target to conclude the importance of SH3-binding domain in favoring mycobacterial growth which can pave the way for translational research advancements in the area of host-directed immunotherapy.

RESOURCE AVAILABILITY

Lead contact

Inquiries and requests for resources should be directed to and will be fulfilled by S.M. (sangita@cdfd.org.in).

Materials availability

Materials generated in this manuscript Msmeg-pVV, Msmeg-MtbCM and Msmeg-MtbCM-PS4 will be available upon request within a reasonable time frame. Please send your inquiries to the designated lead contact.

Data and code availability

- All data generated or analyzed during this study are included in the manuscript and supplementary figures. This paper does not report original code. Any additional information required to reanalyze the data reported in this paper is available from the lead contact upon request.
- This study did not generate any unique datasets or code. Any additional information on data reported in this work is available from the lead contact upon request.

ACKNOWLEDGMENTS

The authors thank Dr. Seyed E Hasnain for his valuable suggestion and discussion. The authors also thank Mr. Niteen Pathak and Mr. Surya Chodisetty for kind help. The laboratory of S.M. is supported by the grants from the Department of Biotechnology (DBT), Govt. of India (BT/PR51149/MED/29/1660/2023), Department of Science and Technology-Science and Engineering Research Board (DST-SERB), Govt. of India (JCB/2021/000035), Council of Scientific and Industrial Research (CSIR), Govt. of India (27(0364)/20/EMR-II); Indian Council of Medical Research, Govt of India ((2021-10087/GTGE/ADHOC-BMS) and a core grant from CDFD by DBT. R.P. was supported by the fellowship from DBT. V.M. and S.B. were supported by DST-INSPIRE Fellowship and DBT-BioCARe Fellowship respectively.

AUTHOR CONTRIBUTIONS

R.P. conceived, performed and wrote the manuscript. V.M. and S.B. worked and performed experiments required for manuscript revision. S.M. conceived the study and provided intellectual, critical feedback, financial resources, manuscript preparation/editing and general guidance.

DECLARATION OF INTERESTS

The authors declare no competing interests.

STAR★METHODS

Detailed methods are provided in the online version of this paper and include the following:

- KEY RESOURCES TABLE
- EXPERIMENTAL MODEL AND STUDY PARTICIPANT DETAILS
  - Animals
  - Isolation of peritoneal macrophages
  - Generation of anti-MtbCM antibody in mice
  - Infection of mice
  - List of antibodies and conjugates used

- Cloning, expression and purification of recombinant MtbCM protein
- Generation of recombinant *M. smegmatis* expressing MtbCM (Msmeg-MtbCM)
- Site-directed mutagenesis of SH3 binding domain in MtbCM
- Detection of MtbCM in bacterial culture
- Growth kinetics
- Cell culture
- Infection of macrophages
- Cytokine assay
- Isolation of golgi fraction
- Pull-down assay
- Transfection of HEK-293T cells
- Immunofluorescence
- Knock-down of AKAP9 by small interfering RNA (siRNA)
- RNA isolation, cDNA synthesis and quantitative real-time PCR (qPCR)
- Intracellular survival assay

- QUANTIFICATION AND STATISTICAL ANALYSIS

SUPPLEMENTAL INFORMATION

Supplemental information can be found online at https://doi.org/10.1016/j.isci.2024.111044.

Received: August 25, 2023
Revised: May 27, 2024
Accepted: September 23, 2024
Published: September 27, 2024

REFERENCES

1. Prakash, P., Aruna, B., Sardesai, A.A., and Hasnain, S.E. (2005). Purified recombinant hypothetical protein coded by open reading frame Rv1885c of *Mycobacterium tuberculosis* exhibits a monofunctional AroQ class of periplasmic chorismate mutase activity. J. Biol. Chem. *280*, 19641–19648. https://doi.org/10.1074/jbc.M413026200.
2. Tohge, T., Watanabe, M., Hoefgen, R., and Fernie, A.R. (2013). Shikimate and phenylalanine biosynthesis in the green lineage. Front. Plant Sci. *4*, 62. https://doi.org/10.3389/fpls.2013.00062.
3. Maeda, H., and Dudareva, N. (2012). The shikimate pathway and aromatic amino Acid biosynthesis in plants. Annu. Rev. Plant Biol. *63*, 73–105. https://doi.org/10.1146/annurev-arplant-042811-105439.
4. Calhoun, D.H., Bonner, C.A., Gu, W., Xie, G., and Jensen, R.A. (2001). The emerging periplasm-localized subclass of AroQ chorismate mutases, exemplified by those from *Salmonella typhimurium* and *Pseudomonas aeruginosa*. Genome Biol. *2*, 1. https://doi.org/10.1186/gb-2001-2-8-research0030.
5. Lambert, K.N., Allen, K.D., and Sussex, I.M. (1999). Cloning and characterization of an esophageal-gland-specific chorismate mutase from the phytoparasitic nematode *Meloidogyne javanica*. Mol. Plant Microbe Interact. *12*, 328–336. https://doi.org/10.1094/MPMI.1999.12.4.328.
6. Degrassi, G., Devescovi, G., Bigirimana, J., and Venturi, V. (2010). *Xanthomonas oryzae* pv. *oryzae* XKK.12 contains an AroQγ chorismate mutase that is involved in rice virulence. Phytopathology *100*, 262–270. https://doi.org/10.1094/PHYTO-100-3-0262.
7. Rollenhagen, C., and Bumann, D. (2006). *Salmonella enterica* highly expressed genes are disease specific. Infect. Immun. *74*, 1649–1660. https://doi.org/10.1128/IAI.74.3.1649-1660.2006.
8. Qamra, R., Prakash, P., Aruna, B., Hasnain, S.E., and Mande, S.C. (2006). The 2.15 A crystal structure of *Mycobacterium tuberculosis* chorismate mutase reveals an unexpected gene duplication and suggests a role in host-pathogen interactions. Biochemistry *45*, 6997–7005. https://doi.org/10.1021/bi0606445.
9. Sasso, S., Ramakrishnan, C., Gamper, M., Hilvert, D., and Kast, P. (2005). Characterization of the secreted chorismate mutase from the pathogen *Mycobacterium tuberculosis*. FEBS J. *272*, 375–389. https://doi.org/10.1111/j.1742-4658.2004.04478.x.
10. Abdalla, A.E., Lambert, N., Duan, X., and Xie, J. (2016). Interleukin-10 family and tuberculosis: An old story renewed. Int. J. Biol. Sci. *12*, 710–717. https://doi.org/10.7150/ijbs.13881.
11. Nair, S., Ramaswamy, P.A., Ghosh, S., Joshi, D.C., Pathak, N., Siddiqui, I., Sharma, P., Hasnain, S.E., Mande, S.C., and Mukhopadhyay, S. (2009). The PPE18 of *Mycobacterium tuberculosis* interacts with TLR2 and activates IL-10 induction in macrophage. J. Immunol. *183*, 6269–6281. https://doi.org/10.4049/jimmunol.0901367.
12. Murray, P.J., and Young, R.A. (1999). Increased antimycobacterial immunity in interleukin-10-deficient mice. Infect. Immun. *67*, 3087–3095. https://doi.org/10.1128/IAI.67.6.3087-3095.1999.
13. Redpath, S., Ghazal, P., and Gascoigne, N.R. (2001). Hijacking and exploitation of IL-10 by intracellular pathogens. Trends Microbiol. *9*, 86–92. https://doi.org/10.1016/s0966-842x(00)01919-3.
14. Flynn, J.L., Goldstein, M.M., Chan, J., Triebold, K.J., Pfeffer, K., Lowenstein, C.J., Schrelber, R., Mak, T.W., and Bloom, B.R. (1995). Tumor necrosis factor-α is required in the protective immune response against *Mycobacterium tuberculosis* in mice. Immunity *2*, 561–572. https://doi.org/10.1016/1074-7613(95)90001-2.
15. Kim, S.K., Reddy, S.K., Nelson, B.C., Vasquez, G.B., Davis, A., Howard, A.J., Patterson, S., Gilliland, G.L., Ladner, J.E., and Reddy, P.T. (2006). Biochemical and structural characterization of the secreted chorismate mutase (Rv1885c) from *Mycobacterium tuberculosis* H37Rv: an *AroQ enzyme not regulated by the aromatic amino acids. J. Bacteriol. *188*, 8638–8648. https://doi.org/10.1128/JB.00441-06.
16. Chauhan, A., Lofton, H., Maloney, E., Moore, J., Fol, M., Madiraju, M.V.V.S., and Rajagopalan, M. (2006). Interference of *Mycobacterium tuberculosis* cell division by Rv2719c, a cell wall hydrolase. Mol. Microbiol. *62*, 132–147. https://doi.org/10.1111/j.1365-2958.2006.05333.x.
17. Cooper, A.M., Mayer-Barber, K.D., and Sher, A. (2011). Role of innate cytokines in mycobacterial infection. Mucosal Immunol. *4*, 252–260. https://doi.org/10.1038/mi.2011.13.
18. Yasui, K. (2014). Immunity against *Mycobacterium tuberculosis* and the risk of biologic anti-TNF-α reagents. Pediatr. Rheumatol. *12*, 45. https://doi.org/10.1186/1546-0096-12-45.
19. Keane, J., Gershon, S., Wise, R.P., Mirabile-Levens, E., Kasznica, J., Schwieterman, W.D., Siegel, J.N., and Braun, M.M. (2001). Tuberculosis associated with infliximab, a tumor necrosis factor α-neutralizing agent. N. Engl. J. Med. *345*, 1098–1104. https://doi.org/10.1056/NEJMoa011110.
20. Gardam, M.A., Keystone, E.C., Menzies, R., Manners, S., Skamene, E., Long, R., and Vinh, D.C. (2003). Anti-tumour necrosis factor agents and tuberculosis risk: mechanisms of action and clinical management. Lancet Infect. Dis. *3*, 148–155. https://doi.org/10.1016/s1473-3099(03)00545-0.
21. Reiling, N., Blumenthal, A., Flad, H.D., Ernst, M., and Ehlers, S. (2001). Mycobacteria-induced TNF-α and IL-10 formation by human macrophages is differentially regulated at the level of mitogen-activated protein kinase activity. J. Immunol. *167*, 3339–3345. https://doi.org/10.4049/jimmunol.167.6.3339.
22. Udgata, A., Qureshi, R., and Mukhopadhyay, S. (2016). Transduction of functionally contrasting signals by two mycobacterial PPE proteins downstream of TLR2 receptors.

J. Immunol. *197*, 1776–1787. https://doi.org/10.4049/jimmunol.1501816.
23. Akita, Y. (2002). Protein kinase C-ε (PKC-ε): its unique structure and function. J. Biochem. *132*, 847–852. https://doi.org/10.1093/oxfordjournals.jbchem.a003296.
24. Kurochkina, N., and Guha, U. (2013). SH3 domains: modules of protein-protein interactions. Biophys. Rev. *5*, 29–39. https://doi.org/10.1007/s12551-012-0081-z.
25. Gelman, I.H. (2002). The role of SSeCKS/gravin/AKAP12 scaffolding proteins in the spaciotemporal control of signaling pathways in oncogenesis and development. Front. Biosci. *7*, d1782–d1797. https://doi.org/10.2741/A879.
26. Belham, C., Wu, S., and Avruch, J. (1999). Intracellular signalling: PDK1–a kinase at the hub of things. Curr. Biol. *9*, R93–R96. https://doi.org/10.1016/s0960-9822(99)80058-x.
27. Cenni, V., Döppler, H., Sonnenburg, E.D., Maraldi, N., Newton, A.C., and Toker, A. (2002). Regulation of novel protein kinase C ε by phosphorylation. Biochem. J. *363*, 537–545. https://doi.org/10.1042/0264-6021:3630537.
28. Limaye, A.J., Bendzunas, G.N., and Kennedy, E.J. (2021). Targeted disruption of PKC from AKAP signaling complexes. RSC Chem. Biol. *2*, 1227–1231. https://doi.org/10.1039/d1cb00106j.
29. Takahashi, M., Mukai, H., Oishi, K., Isagawa, T., and Ono, Y. (2000). Association of immature hypophosphorylated protein kinase cepsilon with an anchoring protein CG-NAP. J. Biol. Chem. *275*, 34592–34596. https://doi.org/10.1074/jbc.M005285200.
30. Global Tuberculosis Report (2023 (World Health Organizatio). https://www.who.int/publications/i/item/9789240083851.
31. Cole, S.T. (2002). Comparative and functional genomics of the *Mycobacterium tuberculosis* complex. Microbiology *148*, 2919–2928. https://doi.org/10.1099/00221287-148-10-2919.
32. Sreejit, G., Ahmed, A., Parveen, N., Jha, V., Valluri, V.L., Ghosh, S., and Mukhopadhyay, S. (2014). The ESAT-6 protein of *Mycobacterium tuberculosis* interacts with beta-2-microglobulin (β2M) affecting antigen presentation function of macrophage. PLoS Pathog. *10*, e1004446. https://doi.org/10.1371/journal.ppat.1004446.
33. Bhat, K.H., Srivastava, S., Kotturu, S.K., Ghosh, S., and Mukhopadhyay, S. (2017). The PPE2 protein of *Mycobacterium tuberculosis* translocates to host nucleus and inhibits nitric oxide production. Sci. Rep. *7*, 39706. https://doi.org/10.1038/srep39706.
34. Pradhan, G., Shrivastva, R., and Mukhopadhyay, S. (2018). Mycobacterial PknG targets the Rab7l1 signaling pathway to inhibit phagosome-lysosome fusion. J. Immunol. *201*, 1421–1433. https://doi.org/10.4049/jimmunol.1800530.
35. Srivastava, S., Battu, M.B., Khan, M.Z., Nandicoori, V.K., and Mukhopadhyay, S. (2019). *Mycobacterium tuberculosis* PPE2 protein interacts with $p67^{phox}$ and inhibits reactive oxygen species production. J. Immunol. *203*, 1218–1229. https://doi.org/10.4049/jimmunol.1801143.
36. Pal, R., Bisht, M.K., and Mukhopadhyay, S. (2022). Secretory proteins of *Mycobacterium tuberculosis* and their roles in modulation of host immune responses: focus on therapeutic targets. FEBS J. *289*, 4146–4171. https://doi.org/10.1111/febs.16369.
37. Sontyana, B., Shrivastava, R., Battu, S., Ghosh, S., and Mukhopadhyay, S. (2022). Phagosome maturation and modulation of macrophage effector function by intracellular pathogens: target for therapeutics. Future Microbiol. *17*, 59–76. https://doi.org/10.2217/fmb-2021-0101.
38. Bhat, K.H., Ahmed, A., Kumar, S., Sharma, P., and Mukhopadhyay, S. (2012). Role of PPE18 protein in intracellular survival and pathogenicity of *Mycobacterium tuberculosis* in mice. PLoS One *7*, e52601. https://doi.org/10.1371/journal.pone.0052601.
39. Feng, C.G., Kullberg, M.C., Jankovic, D., Cheever, A.W., Caspar, P., Coffman, R.L., and Sher, A. (2002). Transgenic mice expressing human interleukin-10 in the antigen-presenting cell compartment show increased susceptibility to infection with *Mycobacterium avium* associated with decreased macrophage effector function and apoptosis. Infect. Immun. *70*, 6672–6679. https://doi.org/10.1128/IAI.70.12.6672-6679.2002.
40. D'Andrea, A., Aste-Amezaga, M., Valiante, N.M., Ma, X., Kubin, M., and Trinchieri, G. (1993). Interleukin 10 (IL-10) inhibits human lymphocyte interferon gamma-production by suppressing natural killer cell stimulatory factor/IL-12 synthesis in accessory cells. J. Exp. Med. *178*, 1041–1048. https://doi.org/10.1084/jem.178.3.1041.
41. Fiorentino, D.F., Zlotnik, A., Vieira, P., Mosmann, T.R., Howard, M., Moore, K.W., and O'Garra, A. (1991). IL-10 acts on the antigen-presenting cell to inhibit cytokine production by Th1 cells. J. Immunol. *146*, 3444–3451.
42. Shin, D.I., Banning, U., Kim, Y.M., Verheyen, J., Hannen, M., Bönig, H., and Körholz, D. (1999). Interleukin 10 inhibits TNF-alpha production in human monocytes independently of interleukin 12 and interleukin 1 beta. Immunol. Invest. *28*, 165–175. https://doi.org/10.3109/08820139909061145.
43. Lyadova, I.V., and Panteleev, A.V. (2015). Th1 and Th17 cells in tuberculosis: Protection, pathology, and biomarkers. Mediators Inflamm. *2015*, 854507. https://doi.org/10.1155/2015/854507.
44. Rook, G.A. (2007). Th2 cytokines in susceptibility to tuberculosis. Curr. Mol. Med. *7*, 327–337. https://doi.org/10.2174/156652407780598557.
45. Rook, G.A.W., Dheda, K., and Zumla, A. (2005). Immune responses to tuberculosis in developing countries: implications for new vaccines. Nat. Rev. Immunol. *5*, 661–667. https://doi.org/10.1038/nri1666.
46. Shaw, T.C., Thomas, L.H., and Friedland, J.S. (2000). Regulation of IL-10 secretion after phagocytosis of *Mycobacterium tuberculosis* by human monocytic cells. Cytokine *12*, 483–486. https://doi.org/10.1006/cyto.1999.0586.
47. Baliko, Z., Szereday, L., and Szekeres-Bartho, J. (1998). Th2 biased immune response in cases with active *Mycobacterium tuberculosis* infection and tuberculin anergy. FEMS Immunol. Med. Microbiol. *22*, 199–204. https://doi.org/10.1111/j.1574-695X.1998.tb01207.x.
48. Kincaid, E.Z., and Ernst, J.D. (2003). *Mycobacterium tuberculosis* exerts gene-selective inhibition of transcriptional responses to IFN-γ without inhibiting STAT1 function. J. Immunol. *171*, 2042–2049. https://doi.org/10.4049/jimmunol.171.4.2042.
49. Ting, L.M., Kim, A.C., Cattamanchi, A., and Ernst, J.D. (1999). *Mycobacterium tuberculosis* inhibits IFN-γ transcriptional responses without inhibiting activation of STAT1. J. Immunol. *163*, 3898–3906.
50. Sodhi, A., Gong, J., Silva, C., Qian, D., and Barnes, P.F. (1997). Clinical correlates of interferon γ production in patients with tuberculosis. Clin. Infect. Dis. *25*, 617–620. https://doi.org/10.1086/513769.
51. Luo, H., Zeng, J., Huang, Q., Liu, M., Abdalla, A.E., Xie, L., Wang, H., and Xie, J. (2016). *Mycobacterium tuberculosis* Rv1265 promotes mycobacterial intracellular survival and alters cytokine profile of the infected macrophage. J. Biomol. Struct. Dyn. *34*, 585–599. https://doi.org/10.1080/07391102.2015.1046935.
52. Parveen, N., Varman, R., Nair, S., Das, G., Ghosh, S., and Mukhopadhyay, S. (2013). Endocytosis of *Mycobacterium tuberculosis* heat shock protein 60 is required to induce interleukin-10 production in macrophages. J. Biol. Chem. *288*, 24956–24971. https://doi.org/10.1074/jbc.M113.461004.
53. Khan, N., Alam, K., Mande, S.C., Valluri, V.L., Hasnain, S.E., and Mukhopadhyay, S. (2008). *Mycobacterium tuberculosis* heat shock protein 60 modulates immune response to PPD by manipulating the surface expression of TLR2 on macrophages. Cell Microbiol. *10*, 1711–1722. https://doi.org/10.1111/j.1462-5822.2008.01161.x.
54. Wilsher, M.L., Hagan, C., Prestidge, R., Wells, A.U., and Murison, G. (1999). Human in vitro immune responses to *Mycobacterium tuberculosis*. Tuber. Lung Dis. *79*, 371–377. https://doi.org/10.1054/tuld.1999.0223.
55. Tu, H., Tang, T.S., Wang, Z., and Bezprozvanny, I. (2004). Association of type 1 inositol 1,4,5-trisphosphate receptor with AKAP9 (Yotiao) and protein kinase A. J. Biol. Chem. *279*, 19375–19382. https://doi.org/10.1074/jbc.M313476200.
56. Horie, K., Ohashi, M., Satoh, Y., and Sairenji, T. (2007). The role of p38 mitogen-activated protein kinase in regulating interleukin-10 gene expression in Burkitt's lymphoma cell lines. Microbiol. Immunol. *51*, 149–161. https://doi.org/10.1111/j.1348-0421.2007.tb03885.x.
57. Singh, P., Rao, R.N., Reddy, J.R.C., Prasad, R., Kotturu, S.K., Ghosh, S., and Mukhopadhyay, S. (2016). PE11, a PE/PPE family protein of *Mycobacterium tuberculosis* is involved in cell wall remodeling and virulence. Sci. Rep. *6*, 21624. https://doi.org/10.1038/srep21624.
58. Balch, W.E., Dunphy, W.G., Braell, W.A., and Rothman, J.E. (1984). Reconstitution of the transport of protein between successive compartments of the Golgi measured by the coupled incorporation of N-acetylglucosamine. Cell *39*, 405–416. https://doi.org/10.1016/0092-8674(84)90019-9.

STAR★METHODS

KEY RESOURCES TABLE

REAGENT or RESOURCE	SOURCE	IDENTIFIER
Antibodies		
Rabbit anti-phospho-PKC ε Ab	Abcam, USA	Cat# Ab88241
Rabbit anti-PKC ε Ab	Abcam, USA	Cat# Ab63638
Mouse anti-phospho-p38 MAPK Ab	BD Biosciences, USA	Cat# 612288
Mouse anti-p38 MAPK Ab	BD Biosciences, USA	Cat# 612169
Rabbit anti-MAPK-1 Ab (DUSP 1)	Abcam, USA	Cat# Ab61201
Rabbit anti-IRAK3 Ab	Cell Signaling Technology, USA	Cat# 4369
Rabbit anti-AKAP9 Ab	Thermo Fisher Scientific, USA	Cat# 360300
Rabbit anti-GAPDH Ab	Abcam, USA	Cat# Ab9485
Anti-GroEL Ab	Gift from Dr S. Mande, NCCS, Pune, India	
Anti-GM130 Ab	Abcam, USA	Cat# Ab52649
Alexa Fluor 488-conjugated goat anti-rabbit Ab	Thermo Fisher Scientific, USA	Cat# A11034
Alexa Fluor 488-conjugated goat anti-mouse Ab	Thermo Fisher Scientific, USA	Cat# A11029
Bacterial and viral strains		
M. smegmatis strain mc^2_{155}	Kind gift from Dr Dipankar Chatterjee, IISC, Bangalore, India	
E. coli BL21 (DE3)	Kind gift from Dr Abhijit A. Sardesai, CDFD, Hyderabad, India	
Chemicals peptides and recombinant proteins		
IPTG (Isopropyl β-D-1-thiogalactopyranoside)	Sigma-Aldrich, USA	Cat# I6758
Freund's Incomplete Adjuvant	Sigma- Aldrich, USA	Cat# F5506
SB203580	Sigma-Aldrich, USA	Cat# S8307
Chorismic acid	Sigma-Aldrich, USA	Cat# C1716
Protease inhibitor cocktail	Roche, Germany	Cat# 04693159001
Lipopolysaccharide (LPS)	Sigma-Aldrich, USA	Cat# L2630
DCP-LA (PKCε Activator)	Sigma-Aldrich, USA	Cat# D5318
siRNA transfection kit		
AKAP9 siRNA Transfection Medium	Santa Cruz Biotechnology	Cat# sc-36868
siRNA Transfection Reagent	Santa Cruz Biotechnology	Cat# sc-29528
Control siRNA-A	Santa Cruz Biotechnology	Cat# sc-37007
Si/shRNA DILUENT RNase free H_2O	Santa Cruz Biotechnology	Cat# NA
AKAP9 siRNA (m)	Santa Cruz Biotechnology	Cat# sc-45365
Critical commercial assays		
Micro BCA™ Protein Assay kit	Thermo Fisher Scientific, USA	Cat# 23235
IL-10 cytokine	BD Biosciences, USA	Cat# 555252
TNF-α cytokine	BD Biosciences. USA	Cat# 555268
Experimental models: cell lines		
RAW 264.7 macrophages		Cat# NA
HEK-293T cells		Cat# NA

(*Continued on next page*)

Continued

REAGENT or RESOURCE	SOURCE	IDENTIFIER
Experimental models: organisms/strains		
Balb/c Mice (Male/Female Any)	CDFD Animal house facility	Cat# NA
Recombinant DNA		
Primers for cloning of MtbCM (F: 5′ ATCATATGTTGCTTACC CGTCCACGTGA 3′ & R: 5′ ATCTCGAGGGCCGG CGGTAGG 3′)	Eurofins	Cat# NA
Primers for Msmeg-MtbCM-PS4 (F: 5′ GCCAGCGCGAGTAGTGAG AGTAGTGATCTATCGGCAT 3′ & R: 5′ CGGTCGCGCGGGGGCCTC GGCGGCCTAGATAGCCGTA 3′)	Eurofins	Cat# NA
Primers for Msmeg-MtbCM (F: 5′ ATCCATATTTGCTTACCC GTCCACGTGA 3′ & R: 5′ ATCGGATCCGAGGGCC GGCGGTAGG 3′)	Eurofins	Cat# NA
Oligonucleotides		
IL-10 cytokine primers (F: 5′ CGGGA AGACAATAACTGCACCC 3′ & R: 5′ CGGTTAGCAGTATGTTGTCCAGC 3′)	Eurofins	Cat# NA
GAPDH primers (F: 5′ CATCACTGC CACCCAGAAGACTG 3′ & R: 5′ ATGCCAGTGAGCTTCCCGTTCAG 3′)	Eurofins	Cat# NA
RPS29 primers (F: 5′ GGTCACCAG CAGCTCTACTG 3′ & R 5′ GTCCAACTTAATGAAGCCTATGTCC 3′)	Eurofins	Cat# NA
Software and algorithms		
Prism 8.0	GraphPad	Cat# NA
ImageJ	Open Source	Cat# NA
Microscopy		
LSM 700 Zeiss confocal microscope	Carl Zeiss Micro-Imaging	Cat# NA

EXPERIMENTAL MODEL AND STUDY PARTICIPANT DETAILS

Animals

Male and female Balb/c mice of 6–8 weeks of age were used for this study. Mice were maintained at the animal house facility of the Center for DNA Fingerprinting and Diagnostics, Hyderabad, and the experimental protocols were performed as per the guidelines of the Institutional Animal Ethics Committee (IAEC).

Isolation of peritoneal macrophages

About 1 mL of 4% thioglycolate was injected intraperitoneally in Balb/c mice. Mice were sacrificed after 4 days using CO_2 asphyxiation. The adherent macrophages were cultured with Dulbecco's Modified Eagle Medium (DMEM) (Invitrogen, USA) supplemented with 10% Fetal Bovine Serum (FBS, Thermo Fisher Scientific, USA), 1% Antibiotic-Antimycotic (Invitrogen, USA) and 1% Glutamax (Invitrogen, USA).

Generation of anti-MtbCM antibody in mice

MtbCM-specific antibody was generated in Balb/c mice as per approved guidelines of the Institutional Animal Ethics Committee (IAEC) of CDFD, Hyderabad. Mice were subcutaneously immunized with recombinant MtbCM (100 μg/mouse) in incomplete Freund's adjuvant (IFA, Sigma Aldrich, USA). After day 21 of the first immunization, two subcutaneously booster doses of the recombinant MtbCM protein

(100 μg/mouse) with IFA were injected at 21-day intervals. On day 73, mice were sacrificed, and sera were collected. The specificity of the MtbCM antibody was confirmed by Western blotting.

Infection of mice

Balb/c mice of 6–8 weeks of age were infected with 5×10^7 CFU of either Msmeg-pVV or Msmeg-MtbCM or Msmeg-MtbCM-PS4 by intravenous injection. To confirm that equal numbers of bacteria were administered, the inoculums were first cultured on 7H10 plates containing antibiotics (kanamycin and hygromycin B) and counted for CFU. At each time point (day 3, 5, and 15), survival of the bacilli in mouse organs was determined using methods as described previously.[57] Briefly, the mice were sacrificed and liver, lung and spleen were removed aseptically and homogenized in sterile PBS-T. Mouse tissue homogenates were diluted in PBS-T and 100 μL aliquots from each dilution were plated on a Middlebrook 7H10 agar plate containing 10% OADC, 25 μg/mL kanamycin, and 50 μg/mL of hygromycin B. The plates were incubated at 37°C and the CFUs were determined after 4 days.

List of antibodies and conjugates used

Rabbit anti-PKC epsilon (phospho S729) antibody (Ab) (Abcam, USA), rabbit anti-PKCε Ab (Abcam, USA), mouse anti-phospho-p38 MAPK Ab (BD Biosciences, USA), mouse anti-p38 MAPK Ab (BD Biosciences, USA), rabbit anti-MKP-1 Ab (Abcam, USA), rabbit anti-IRAK3 Ab (Cell Signaling Technology, USA), rabbit anti-AKAP9 Ab (Thermo Fisher Scientific, USA), anti-GAPDH mouse Ab (Abcam, USA), Alexa Fluor 488-conjugated goat anti-rabbit Ab (Thermo Fisher Scientific, USA), Alexa Fluor 488-conjugated goat anti-mouse Ab (Thermo Fisher Scientific, USA).

Cloning, expression and purification of recombinant MtbCM protein

The MtbCM was amplified from *M. tuberculosis* H37Rv genomic DNA using specific set of primer pair (Forward Primer; 5′-ATC ATATGTTGCTTACCCGTCCACGTGA-3′ and Reverse primers; 5′- ATCTCGAGGGCCGGCGGTAGG-3′). Amplification was carried out using a thermal cycler with denaturation at 95°C, annealing at 61°C, and extension at 72°C for 30 cycles. The polymerase PCR products were cloned into the corresponding sites of the pET23a (Novagen, USA) expression vector containing 6X-His-tag at the C-terminus. *E. coli* BL21(DE3) cells were transformed with pET23a-MtbCM and were grown in 1 L of LB (Luria-Bertani) liquid medium supplemented with 100 μg/mL ampicillin and 10% glycerol. To induce protein expression, Isopropyl β-D-1-thiogalactopyranoside (IPTG) was added to the mid-log phase culture at a final concentration of 0.1 mM. The cells were incubated at 27°C/150 rpm for 5 h in an incubator shaker to allow protein expression. Following induction, the cells were harvested by centrifugation and re-suspended in lysis buffer (10 mM Tris-HCl, 100 mM NaCl, and 10% glycerol, pH 7.5) with 0.1 mM phenylmethylsulfonyl fluoride (PMSF) and disrupted using a sonicator. After another round of centrifugation for 10 min at 10,000 × g, the supernatant was applied to a Talon cobalt affinity resin (Clontech, USA). The nonspecific proteins were removed by washing the column with 5-bed volume of lysis buffer containing 30 mM imidazole. The desired protein fractions were eluted with lysis buffer containing 300 mM imidazole. The fractions containing protein were collected, pooled, and dialyzed against PBS buffer to remove salts and imidazole. The purity of the protein was checked by SDS-PAGE followed by Coomassie Brilliant Blue staining.

Generation of recombinant *M. smegmatis* expressing MtbCM (Msmeg-MtbCM)

MtbCM was amplified from *M. tuberculosis* H37Rv genomic DNA using a specific set of primers (Forward primer; 5′-ATC CATATTTGCTTACCCGTCCACGTGA-3′ and reverse primer; 5′ -ATCGGATCCGAGGGCCGGCGGTAGG-3′. The PCR products were cloned into the corresponding NdeI and BamHI sites of pVV16 vector containing 6 histidine-tag (6X-His-tag) at its C-terminus. The presence of MtbCM sequence in the frame was further confirmed by sequencing the recombinant clones (pVV16-MtbCM). *M. smegmatis* competent cells were transformed with pVV16-MtbCM via electroporation. Positive transformants were selected on Middlebrook 7H10 agar plates containing 10% OADC (Oleic Albumin Dextrose Catalase, HIMEDIA, India), kanamycin (25 μg/mL), and hygromycin B (50 μg/mL). Single bacterial colonies were picked up and MtbCM expression was confirmed by immunoblotting using anti-MtbCM Ab raised in-house in mice (Balb/c).

Site-directed mutagenesis of SH3 binding domain in MtbCM

Site-directed mutagenesis was performed by using primers containing the required mutations. To mutate all four proline to serine residues of the SH3 binding motif of MtbCM, the set of primers (forward Primer; 5′- GCCAGCGCGAGTAGTGAGAGTAGTGATCTATCGGCAT-3′ and reverse Primer; 5′- CGGTCGCGCGGGGGCCTCGGCGGCCTAGATAGCCGTA-3′). The primers were used to amplify the whole pVV16-MtbCM plasmid. The template plasmid was digested using Dpn1 enzyme and the mixture was transformed into XL-1 Blue comp cells. The selected mutants (MtbCM-PS4) were confirmed by DNA sequence analysis. Next, *M. smegmatis* competent cells were transformed with pVV16-MtbCM-PS4 via electroporation. Positive transformants were selected on Middlebrook 7H10 agar plates containing 10% OADC, kanamycin (25 μg/mL), and hygromycin B (50 μg/mL). Single bacterial colonies were picked and MtbCM-PS4 expression was confirmed by immunoblotting using anti-MtbCM Ab.

Detection of MtbCM in bacterial culture

Msmeg-MtbCM was grown in Sauton's medium with kanamycin (25 μg/mL) and hygromycin (50 μg/mL). Once the culture reached absorbance at 600 nm to 0.8–1.0, the culture filtrate (CF) was harvested by centrifugation, and CF was filtered using 0.45-micron filter. Next, the CF was

concentrated about 200 times using a 3 kDa cut-off centricon filter (Millipore, USA) at 4°C. Concentrated CF was mixed with 1X Laemmli buffer and boiled at 95°C for 5–10 min. The bacterial cell lysate was also prepared by sonicating the pellets in lysis buffer [10 mM Tris-HCl, 100 mM NaCl, and 10% glycerol, pH 7.5) with 0.1 mM phenylmethylsulfonyl fluoride (PMSF)] and mixed with 1X Laemmli buffer and boiled at 95°C for 5–10 min. Next, bacterial cell lysate and CF were resolved on SDS-PAGE followed by Western blotting using anti-MtbCM antibody and HRP (horseradish peroxidase) conjugated anti-mouse secondary Ab (Sigma-Aldrich, USA). GroEL1 was used as a negative control for bacterial cell lysis.

Growth kinetics

Colonies of Msmeg-MtbCM or *M. smegmatis* harboring the empty vector alone (pVV16) (Msmeg-pVV) were inoculated in 10 mL 7H9 broth to prepare the primary inoculum. About 1 mL of the primary culture of either Msmeg-pVV or Msmeg-MtbCM containing 100 million bacteria was inoculated into 100 mL of secondary culture. Absorbance at 600 nm was measured every 4 h till the culture reached to stationary phase. Growth rate (r) was calculated using the formula:

$$r = (\ln [\text{Absorbance 2} / \text{Absorbance 1}]) / (T2 - T1)$$

Where Absorbance 1 and Absorbance 2 indicate the absorbance measured at time T1 and T2 respectively.

Cell culture

RAW 264.7 macrophages and HEK-293T cells were cultured in DMEM supplemented with 10% Fetal Bovine Serum (FBS), 1% Antibiotic-Antimycotic and 1% Glutamax. The cells were not authenticated internally, as they were pre-authenticated by a non-profit organization (ATCC). Additionally, both cell lines were confirmed to be free of mycoplasma contamination.

Infection of macrophages

RAW 264.7 macrophages cultured in antibiotic-free medium were infected with either Msmeg-MtbCM or Msmeg-pVV or Msmeg-MtbCM-PS4 at the multiplicity of infection (MOI) of 1:10 or 1:50. After 2 h of infection, cells were washed to remove extracellular bacilli. Cells were further incubated at various time points for carrying out different experiments. Culture supernatants were harvested for measuring cytokines after 24 h and 48 h of infection.

Cytokine assay

The interleukin-10 (IL-10) and tumor necrosis factor-alpha (TNF-α) cytokines secreted in the macrophage culture supernatants, tissue lysates and blood sera of infected mice were quantified by two-site sandwich enzyme immunoassay (EIA) following the manufacturer's protocol (BD Biosciences, USA) as described earlier.[11]

Isolation of golgi fraction

Golgi fractions were isolated as described earlier.[34,58] About 120 million RAW 264.7 macrophages were infected with either Msmeg-pVV or Msmeg-MtbCM with MOI 1:50. After 5 h of infection, cells were washed and resuspended in lysis buffer (10 mM Tris-HCl, pH 7.4; 250 mM sucrose; 20 mM EDTA, pH 8.0 and protease inhibitor cocktail). The lysate was centrifuged at 5,000 rpm for 10 min to isolate the post-nuclear supernatant (PNS). PNS was resuspended with 62% of sucrose to a final concentration of 37% w/v and is poured as the first layer in the ultra-centrifuge tube followed by 35% and 29% sucrose solution. The tubes were centrifuged at 100,000 × g for 2.5 h. The Golgi fractions were isolated from the band appearing between the interface of 35% and 29% sucrose gradient.

Pull-down assay

RAW 264.7 macrophages were infected with either Msmeg-pVV or Msmeg-MtbCM or Msmeg-MtbCM-PS4 at MOI of 1:50. After 5–6 h of infection, infected cells were harvested, and the lysates were prepared using a lysis buffer containing 50 mM Tris; 100 mM NaCl; 1% NP-40; 1X Protease inhibitor cocktail (Roche, Germany); 1 mM PMSF and 1X phosphatase (Sigma-Aldrich, USA). The lysate was further incubated with 1 μg of anti-AKAP9 Ab overnight at 4°C. The next day, lysate was incubated with Protein A/G beads (Santa Cruz, USA) at 4°C and after 2 h of incubation, beads were pelleted down and washed with lysis buffer. After washing, beads were incubated with 1X Laemmli buffer and boiled at 95°C for 5–10 min. Next, beads were loaded onto 10% SDS-PAGE followed by Western blotting using anti-MtbCM Ab or anti-PKCε Ab.

Transfection of HEK-293T cells

HEK-293T cells were transiently transfected using Lipofectamine 2000 (Invitrogen, USA) using the manufacturer's protocol. Briefly, for co-transfection, 0.5 μg of each plasmid and 3 μL of Lipofectamine 2000 mixture were diluted separately in 100 μL of Opti-MEM (Invitrogen, USA) and incubated at room temperature. After 20 min of incubation, the mixture was added to HEK-293T cells and cultured in Opti-MEM. After 6 h of transfection, cells were replenished with fresh complete DMEM medium and after 24 h of transfection cells were harvested for further experiments.

Immunofluorescence

RAW 264.7 macrophages were infected with either Msmeg-MtbCM of Msmeg-pVV at MOI of 1:10. Cells were harvested and were fixed with 4% paraformaldehyde solution for 15 min. Next cells were washed with PBS and permeabilized using PBS containing 0.15% Triton X-100 (Sigma-Aldrich, USA) for another 15 min. After permeabilization, blocking was carried out using 5% BSA in PBS for 2 h. After blocking, cells were incubated with primary Ab overnight at 4°C. Next cells were washed and incubated with Alexa Fluor 488–conjugated secondary Ab (Molecular Probes, USA) for 60 min. Cells were washed and mounted with an antifade mounting medium with DAPI (Vector Labs, USA) and observed under LSM 700 Zeiss confocal microscope (Carl Zeiss Micro-Imaging).

HEK-293T cells transfected with either a combination of mCherry-TGOLN2 and pEGFP (pEGFP-N1) or mCherry-TGOLN2 and pEGFP-MtbCM were harvested after 24 h post-transfection. Cells were washed with PBS and were fixed using a 4% paraformaldehyde solution. Next cells were washed and mounted with an antifade mounting medium with DAPI. Cells were visualized under LSM 700 Zeiss confocal microscope.

Knock-down of AKAP9 by small interfering RNA (siRNA)

Knock-down of AKAP9 in RAW 264.7 macrophages were performed using mouse specific AKAP9 siRNA (sc-45365) following the manufacturer's protocol (Santa Cruz Biotechnology, USA). The control group received non-targeting siRNA (sc-37007). Briefly, for 12 well plate, 60 pmol siRNA duplex was diluted in siRNA Transfection Medium (3 μL in 200 μL, sc-36868). The siRNA Transfection Reagent (sc-29528) was also diluted in transfection medium (3 μL in 200 μL) and both the solutions were mixed and incubated for 30 min at room temperature. The mixture was then added to the cells in a serum free medium for 5 h following which FBS was added. After 24 h, cells were harvested to check the level of AKAP9 protein expression in control (AKAP-CT) and AKAP9 knock-down (AKAP-KD) macrophages by Western blotting using anti-AKAP9 Ab.

RNA isolation, cDNA synthesis and quantitative real-time PCR (qPCR)

Cells were homogenised in the Trizol solution (Ambion, USA) for RNA isolation, and chloroform was added. After brief vortexing and incubation for 2–3 min at room temperature, the samples were centrifuged, and transparent supernatant was collected. An equal amount of isopropanol was added, and the mixture was centrifuged for 30 min at 14000 rpm (4°C). The pellets were washed twice with 70% ethanol at 14000 rpm (4°C) for 15 min. The pellet was air-dried and dissolved in nuclease-free water. The RNA quantity and quality were analyzed by Nanodrop. cDNA synthesis was carried out using Moloney Murine Leukemia Virus (M-MLV) reverse transcriptase or SuperScript III reverse transcriptase as per the manufacturer's protocol (Invitrogen, USA). Real-time PCR for IL-10 was carried out with primers (Forward primer; 5′-CGGGAAGACAATAACTGCACCC-3′; and Reverse primer; 5′-CGGTTAGCAGTATGTTGTCCAGC-3′) using CFX96 Real-time PCR system (Bio-Rad, USA) with DyNamo flash SYBR GREEN qPCR master mix (Invitrogen, USA) for detection. The fold change ($2^{-\Delta\Delta Ct}$) method was used to calculate the differential rate of transcription using CFX Maestro Software (Bio-Rad, USA). GAPDH (Forward primer; 5′- CATC ACTGCCACCCAGAAGACTG-3′: and Reverse Primer; 5′- ATGCCAGTGAGCTTCCCGTTCAG-3′) or RPS29 (Forward primer; 5′-GGTCAC CAGCAGCTCTACTG-3′ and Reverse primer; 5′-GTCCAACTTAATGAAGCCTATGTCC-3′) transcript level was used as the internal control.

Intracellular survival assay

For *ex vivo* intracellular survival assay, RAW 264.7 macrophages were infected with either Msmeg-MtbCM or Msmeg-pVV or Msmeg-MtbCM-PS4 at MOI of 1:10. Next, macrophages were harvested at various time points (3 h, 24 h, 48 h), lysed, and plated over 7H10 agar supplemented with 10% Middlebrook OADC, 25 μg/mL kanamycin and 50 μg/mL hygromycin B for determining intracellular viable bacteria by colony-forming unit (CFU) counting.

QUANTIFICATION AND STATISTICAL ANALYSIS

Data are presented as Mean ± SEM, and Student's *t*-test was used to determine the statistical significance of differences between the groups. $p < 0.05$ was considered to be significant.